Impulsive observer with predetermined finite convergence time for synchronization of fractional-order chaotic systems based on Takagi–Sugeno fuzzy model

Said Djennoune · **Maamar Bettayeb** ·
Ubaid Mohsen Al Saggaf

Abstract This paper is devoted to the problem of observer design for synchronization of nonlinear fractional-order chaotic systems described by the Takagi–Sugeno fuzzy model. We propose a new method of designing an observer that converges in finite time. The novelty of the proposed observer compared to those developed in the literature is that the estimated state exactly converges to the true state in a finite time which can be chosen beforehand. This is made possible by updating the estimated state at a defined time instant. The abrupt update shows up an impulsive behavior of the observer's dynamics. Two cases are considered. In the first case, the system is not affected by an unknown input. The second case considers the system subjected to the action of an unknown input. Finite-time convergence of the two proposed observers for both cases is established using linear matrix inequality formulation.

S. Djennoune (✉)
Laboratoire de Conception et Conduite de Systemes de Production, University Mouloud Mammeri, Tizi-Ouzou, Algeria
e-mail: s_djennoune@yahoo.fr

M. Bettayeb
Department of Electrical and Computer Engineering, University of Sharjah, Sharjah, UAE

M. Bettayeb · U. M. Al Saggaf
Center of Excellence in Intelligent Engineering Systems (CEIES), King Abdulaziz University, Jeddah, Kingdom of Saudi Arabia

U. M. Al Saggaf
Electrical and Computer Engineering Department, King Abdulaziz University, Jeddah, Kingdom of Saudi Arabia

Simulation results on the synchronization of fractional-order chaotic systems clearly illustrate the impulsive behavior of the proposed observer and the predefined finite-time synchronization. The advantage of predefined finite-time synchronization is highlighted by the ability of recovering an encrypted message without loss of information in a fractional-order chaos-based secure communication application.

1 Introduction

Fractional-order systems have gained more and more attention in various application fields in several branches of science and engineering [1–3]. It is recognized that fractional calculus is a powerful mathematical tool for modeling with more accuracy some complex physical phenomena such as dielectric polarization [4], heat conduction [5], viscoelasticity material [6] and electrical circuits [7]. On the other hand, the introduction of fractional-order controllers, instead of conventional PID controllers [3,8], has greatly improved the robustness of the control system.

The phenomenon of chaos in fractional-order nonlinear systems has also been an exciting topic [9,10]. Fractional-order chaotic systems improve the security level of cryptosystems because of their complex

dynamics and by the fact that fractional orders of derivatives are used as additional parameters to the security key space [11–13]. Indeed, the encryption of a secret message by a fractional-order chaotic system complicates the recovering of the message by a possible intruder. In secure communication systems based on fractional-order chaos, the transmitter is a chaotic system of fractional order. The secret information is masked by modulation in the incomprehensible fractional-order chaotic signal that is sent to the receiver via the public channel. At the receiver, the secret message is retrieved by the demodulation operation. The recovery of the secret message is only possible after synchronization of the receiver and the emitter is achieved. So, in the design of chaos-based cryptographic systems, the problem of synchronization is crucial. Thanks to the remarkable work of Caroll and Pecora [14], two chaotic systems can be synchronized despite their sensitivity to the initial conditions and their unpredictable behavior.

Synchronization methods for two fractional-order chaotic systems developed in the literature are numerous and very varied such as projective synchronization [15,16], adaptive schemes [17], cascade synchronization method [18], optimal approach [19], impulsive methods [20,21] and active control strategy [22]. In the same spirit, the synchronization problem has also been addressed for complex neural network fractional-order systems [23,24].

Among the many methods of synchronization of fractional-order chaotic systems, observer-based methods, highlighted by the work of Niejemeejer and Mareels [25], have led to a large number of contributions. A proportional integral observer is proposed in [26] for synchronization of two fractional-order chaotic systems. A fractional-order high-gain observer is designed for fractional-order nonlinear systems subject to delayed measurements [27]. Nonlinear observer has been addressed in [28] to achieve projective synchronization. Sliding mode observers have been widely applied to nonlinear fractional-order systems; for instance, see recent published works [29–34] and references cited therein.

As rightly pointed out recently in [35], it should be noted that many observer design techniques dedicated to chaotic synchronization converge asymptotically. Although approaches based on sliding modes and homogeneous functions guarantee convergence in finite time [36], the convergence time is not known and

remains dependent on the system initial conditions; this is usually an unbounded function of the initial conditions. Increasing the speed of convergence with this type of observer requires high-gain output injection. Unfortunately, the use of discontinuous high-gain output injection induces severe drawbacks such as chattering phenomenon, transient peaks with high amplitude and high sensitivity to measurement noise [37].

In secure transmission scheme design, asymptotic convergence is undesirable because significant delays for synchronization render the recovering of the confidential message a very hard task. A loss of information can corrupt the transmission of the message especially if the first samples of the information constitute confidential signaling data. In such application, the use of finite-time synchronization methods is essential. We must therefore design state observers that converge in a finite time. For the best synchronization, the ideal solution is to design state estimators that exactly converge without estimation error and in a time preselected in advance. Knowing exactly the synchronization delay, it is then possible to carry out the transmission without any loss of information either by delaying the sending of the message until the synchronization is established or by adding to the beginning of the confidential message another information without any meaning.

In [35], the authors considered this important point in the case of synchronization of integer-order chaotic systems. Even if the convergence time is fixed arbitrary, however, its predetermined value must be greater than a lower limit depending on the system initial conditions. To the best of our knowledge, the finite-time synchronization with a predefined time of convergence has never been addressed for fractional-order chaotic systems.

Motivated by the above discussion, the objective of our work is twofold. On the one hand, considering the importance of fractional-order chaotic systems in the design of secure communication schemes, we propose an innovative solution for finite-time synchronization of fractional-order chaotic systems. On the other hand, the solution that we propose allows to arbitrarily choose in advance the convergence time independently on the system initial conditions.

The key idea of the solution we propose is based on the impulsive observer developed by Raff and Allgower [38,39] for integer-order linear continuous-time systems. The principle of the Raff's continuous-time deadbeat observer consists in a abrupt update of the

estimated state at a definite time instant chosen in advance. An exact convergence is then obtained in finite time thanks to an update gain computed from the transition matrix of the system. Recently, the Raff's idea has been extended to fractional-order linear systems in [40]. However, the extension of the Raff's observer to nonlinear systems of both integer order and fractional order is not obvious. Indeed, it remains difficult to determine the update gain which is the key element of the Raff's observer since, for general nonlinear systems, the notion of transition matrix is not defined. In order to solve this problem, we propose to represent the nonlinear system in the form of a fuzzy Takagi–Sugeno (T–S) model consisting of a weighted superposition of several linear local sub-models. The fuzzy T–S model was introduced first by Takagi and Sugeno [41]. It is therefore possible to use the tools of linear systems to design local observers corresponding to each linear subsystem. There exist many methods that can be used in order to obtain the fuzzy T–S model for a given nonlinear system. The linearization method consists of summing linear models obtained around some operating points with judicious weighting functions. The black box identification-based method imposes, in advance, the T–S structure and then proceeds to the estimation of the T–S structure parameters [42]. The third method makes it possible to obtain an exact representation T–S for any nonlinear system at least in a compact state space. This method is based on the nonlinear sector transformations [43,44]. The T–S fuzzy representation of integer-order nonlinear systems had a considerable impact on observers design [45,46]. Similarly, some works have been devoted to controllers' and observers' design for nonlinear fractional-order systems using T–S fuzzy models including observer-based synchronization of fractional-order chaotic systems; for instance, see some recent published papers [47–52].

Our contribution is based on two guiding ideas. The first one is to use the T–S representation for fractional-order nonlinear systems. The second one is to develop an extension of the Raff's impulsive observer with a predetermined convergence time to the synchronization of fractional-order chaotic systems described by T–S models. We consider two cases. In the first case, the system is not affected by an unknown input. The second case considers the system subjected to the action of an unknown input. This second case is part of the design of fractional-order chaotic system-based secure commu-

nication schemes. The unknown input represents the secret message to be transmitted. In both cases, we show that the estimated state exactly converges to the true state in a finite time which can be chosen almost arbitrarily. This is made possible by an impulsive updating process of the estimated state, at a desired time. This advantage is efficiently illustrated in the synchronization of two fractional-order chaotic systems used in a secure data communication scheme.

The rest of the paper is organized as follows. In Sect. 2, definitions on fractional-order systems are given. The problem statement and the aim goal of the present work are presented. Moreover, preliminary stability results on T–S fuzzy fractional-order systems are derived. In Sect. 3, the proposed finite convergence time impulsive observer for T–S fuzzy fractional-order systems is designed. First, we consider that the system is not subjected to an unknown input, while in the second step, the presence of an unknown input is taken into account. This second case reflects the application of the proposed observer to secure communication in which the unknown input represents the secret message to be confidentially sent from the emitter to the receiver. For both cases, the finite-time convergence is established by using linear matrix inequality (LMI) stability results of fractional-order systems [53–56]. Section 4 is devoted to numerical application of the proposed observer to the synchronization of two fractional-order chaotic systems in a secure data communication scheme.

Notations

Throughout this paper, the following standard notations are used. $\mathbb{R}^n$ and $\mathbb{R}^{n \times m}$ denote the n-dimensional Euclidean space and the set of $n \times m$ real matrices, respectively. $\mathbb{R}_+^*$, $\mathbb{R}_+$ and $\mathbb{N}$ represent the strictly positive real numbers set, the nonnegative real numbers set and the integer numbers set, respectively. For a real matrix M, the notation M^{T} represents the transpose of M. I_n and $0_{n \times m}$ denote the $n \times n$ identity matrix and the $n \times m$ null matrix, respectively. For a given real symmetric matrix X, the inequalities $X < 0$ ($X \leq 0$) and $X > 0$ ($X \geq 0$) indicate that X is negative (semi) definite and positive (semi) definite, respectively. The symbol $\mathrm{Sym}(M)$ means $M + M^{\mathrm{T}}$ and the conventional notation $A \otimes B$ denotes the Kronecker product between the two matrices A and B. The symbol $(*)$ in the follow-

ing partitioned symmetric matrix $\begin{bmatrix} A & B \\ (*) & C \end{bmatrix}$ denotes the symmetric item, i.e., $(*) = B^{\mathrm{T}}$.

2 Problem formulation and preliminary results

In the field of fractional-order systems modeling and control, several fractional derivative definitions have been introduced. Among these, the Caputo's definition is advantageous because the solution of the corresponding differential equations depends on the initial conditions defined in classical ways that makes it applicable to physical systems [57,58]. Throughout this paper, we adopt the Caputo's fractional derivative defined as follows.

Definition 1 [57] The Caputo derivative of a given real order $\alpha \in \mathbb{R}_+^*$, $\ell - 1 < \alpha < \ell$, $\ell \in \mathbb{N}$ on a real-valued function $f(t)$ with respect to the variable $t \in \mathbb{R}_+$ which represents the time is defined as

$$D^\alpha f(t) = \frac{1}{\Gamma(\ell - \alpha)} \int_{t_0}^t \frac{1}{(t - \tau)^{\alpha + 1 - \ell}} \frac{\mathrm{d}^\ell f(\tau)}{\mathrm{d}\tau^\ell} \mathrm{d}\tau \quad (1)$$

where t_0 denotes the initial time and the Euler's gamma function $\Gamma(\alpha)$ is defined as

$$\Gamma(\alpha) = \int_0^\infty \nu^{\alpha - 1} e^{-\nu} \mathrm{d}\nu \quad (2)$$

In the present work, we focus mainly on the case of $0 < \alpha < 1$. Nevertheless, we also give some results for the case $1 \le \alpha < 2$.

Definition 2 [57,58]. The α-order Riemann–Liouville integral operator on a real-valued function $f(t)$ is expressed as follows.

$$I^\alpha f(t) = \frac{1}{\Gamma(\alpha)} \int_{t_0}^t \frac{1}{(t - \tau)^{1 - \alpha}} f(\tau) \mathrm{d}\tau \quad (3)$$

Let us recall below some useful results related to the stability and observability of commensurate fractional-order linear systems described by

$$\begin{aligned} D^\alpha x(t) &= Ax(t) + Bu(t) \\ y(t) &= Cx(t) \end{aligned} \quad (4)$$

where $x(t) = [x_1(t) \quad x_2(t) \quad \dots \quad x_n(t)]^{\mathrm{T}} \in \mathbb{R}^n$ is the n-dimensional state vector, $u(t) \in \mathbb{R}^m$ the input control vector and $y(t) \in \mathbb{R}^p$ the output vector. A, B and C are constant real matrices with appropriate dimensions and $0 < \alpha < 1$. Let t_0 be the initial time and $x_0 = x(t_0)$

the initial condition. The solution of (4) is given by [57,58].

$$\begin{aligned} x(t) &= E_\alpha \left(A(t - t_0)^\alpha \right) x_0 \\ &\quad + \int_{t_0}^t (t - \tau)^{\alpha - 1} E_{\alpha,\alpha} \left(A(t - \tau)^\alpha \right) Bu(\tau) \mathrm{d}\tau \end{aligned}$$
$$(5)$$

where $E_\alpha \left(A(t - t_0)^\alpha \right)$ represents the Mittag–Leffler function defined as [57],

$$E_\alpha(At^\alpha) = \sum_{k=0}^\infty \frac{A^k t^{k\alpha}}{\Gamma(1 + k\alpha)} \quad (6)$$

and $E_{\alpha,\beta} \left(At^\alpha \right)$ denotes the two parameters Mittag–Leffler function defined as

$$E_{\alpha,\beta}(At^\alpha) = \sum_{k=0}^\infty A^k \frac{t^{k\alpha}}{\Gamma(k\alpha + \beta)} \quad (7)$$

For integer-order systems, asymptotic stability is characterized by an exponential decay of its solution, i.e., the asymptotically stable system is said to be exponentially stable. However, for fractional-order systems, the asymptotically stability is characterized by the Mittag–Leffler stability defined as follows [56].

Definition 3 The solution of the fractional-order system $D^\alpha x(t) = f(t, x)$ is said to be Mittag–Leffler asymptotically stable if for any initial condition $x_0 = x(t_0)$, there exist positive constants $\lambda \ge 0$, $\rho > 0$ such that $\|x(t)\| \le \{\nu(x_0) E_\alpha \left(-\lambda (t - t_0)^\alpha \right)\}^\rho$, for all $t \ge t_0$ with $\nu(0) = 0$, $\nu(x) \ge 0$ and $\nu(x)$ is locally Lipschitz on $x \in \mathbb{D} \subset \mathbb{R}^n$.

A special case of the Mittag–Leffler stability is the power-law stability defined as follows [54,59].

Definition 4 The solution of the fractional-order system $D^\alpha x(t) = f(t, x)$ is said to be $t^{-\beta}$ asymptotically stable if for any initial condition $x_0 = x(t_0)$, there exists a positive real β such that

$$\forall \|x(t)\|, \quad t \le t_0, \quad \exists \vartheta(x(t), \quad t \le t_0), t_1(x(t), t \le t_0)$$

such that

$$\forall t > t_0, \quad \|x(t)\| \le \vartheta(t - t_1)^{-\beta}$$

Remark 1 For fractional-order systems, the trajectories slowly decay toward 0 following $t^{-\beta}$ which reflects the long memory phenomenon of fractional-order systems.

One of the first stability results for fractional-order linear systems is due to D. Matignon and is stated in the following lemma.

Lemma 1 [59] *The fractional-order linear system* (4) *with* $0 < \alpha < 2$ *is asymptotically stable if and only if*

$$|\text{Arg}(\text{spec}(A))| > \alpha \frac{\pi}{2} \tag{8}$$

where $\text{spec}(A)$ *denotes the set of all eigenvalues, including repeated eigenvalues of* A *and* Arg, *which denote the argument of a complex number.*

The Lyapunov-based stability result of fractional-order linear systems is formulated by the following lemma.

Lemma 2 [53] *The fractional-order linear system* (4) *with* $0 < \alpha < 1$ *is asymptotically stable if and only if there exist two real symmetric positive definite matrices* $P_{k1} \in \mathbb{R}^{n \times n}$, $(k = 1, 2)$ *and two real skew symmetric matrices* $P_{k2} \in \mathbb{R}^{n \times n}$, $(k = 1, 2)$, *such that*

$$\sum_{k=1}^{2} \sum_{\ell=1}^{2} \text{Sym} \left\{ \Theta_{k\ell} \otimes \left(A^{\text{T}} P_{k\ell} \right) \right\} < 0 \tag{9}$$

$$\begin{bmatrix} P_{11} & P_{12} \\ -P_{12} & P_{11} \end{bmatrix} > 0, \quad \begin{bmatrix} P_{21} & P_{22} \\ -P_{22} & P_{21} \end{bmatrix} > 0, \tag{10}$$

where

$$\Theta_{11} = \begin{bmatrix} \sin(\theta) & -\cos(\theta) \\ \cos(\theta) & \sin(\theta) \end{bmatrix},$$

$$\Theta_{12} = \begin{bmatrix} \cos(\theta) & \sin(\theta) \\ -\sin(\theta) & \cos(\theta) \end{bmatrix} \tag{11}$$

$$\Theta_{21} = \begin{bmatrix} \sin(\theta) & \cos(\theta) \\ -\cos(\theta) & \sin(\theta) \end{bmatrix},$$

$$\Theta_{12} = \begin{bmatrix} -\cos(\theta) & \sin(\theta) \\ -\sin(\theta) & -\cos(\theta) \end{bmatrix} \tag{12}$$

with $\theta = \alpha \frac{\pi}{2}$.

Analog result is established for the case of $1 \leq \alpha < 2$ and is given below.

Lemma 3 [54] *The fractional-order linear system* (4) *with* $1 \leq \alpha < 2$ *is asymptotically stable if and only if there exists a real symmetric positive definite matrix* $P \in \mathbb{R}^{n \times n}$ *such that*

$$\begin{bmatrix} (A^{\text{T}} P + P A)\sin(\tilde{\theta}) & (A^{\text{T}} P - P A)\cos(\tilde{\theta}) \\ (*) & (A^{\text{T}} P + P A)\sin(\tilde{\theta}) \end{bmatrix} < 0 \tag{13}$$

or equivalently

$$\text{Sym} \left(\tilde{\Theta} \otimes (A^{\text{T}} P) \right) < 0 \tag{14}$$

where $\tilde{\theta} = \pi - \alpha \frac{\pi}{2}$ *and*

$$\tilde{\Theta} = \begin{bmatrix} \sin(\tilde{\theta}) & \cos(\tilde{\theta}) \\ -\cos(\tilde{\theta}) & \sin(\tilde{\theta}) \end{bmatrix} \tag{15}$$

The observability condition of the fractional-order system (4) is stated in the following theorem.

Theorem 1 [60] *System* (4) *is observable if and only if the following Kalman's rank condition*

$$\text{rank} \begin{bmatrix} C \\ CA \\ CA^2 \\ \vdots \\ CA^{n-1} \end{bmatrix} = n \tag{16}$$

is fulfilled.

Another useful result for the statement of our main contribution concerns the solution of time-varying fractional-order systems [61,62].

Definition 5 The transition matrix $\Phi(t, t_0)$ of the following time-varying fractional-order system

$$D^{\alpha} x(t) = A(t) x(t) \tag{17}$$

is defined as the unique solution of the fractional-order differential equation

$$D^{\alpha} \Phi(t, t_0) = A(t) \Phi(t, t_0), \quad \Phi(t_0, t_0) = I_n \tag{18}$$

The solution of (17) for a initial condition $x_0 = x(t_0)$ is given by

$$x(t) = \Phi(t, t_0) x_0 \tag{19}$$

Lemma 4 *The state transition* $\Phi(t, t_0)$ *of* (17) *with* $0 < \alpha < 1$ *is expressed by* [61,62]

$$\Phi(t, t_0) = \sum_{k=0}^{\infty} I_{t_0, t}^{k \circ \alpha} A(t) \tag{20}$$

where

$$I_{t_0, t}^{0 \circ \alpha} A(t) = I_{t_0, t}^{0} A(t) = I_n$$

$$I_{t_0, t}^{1 \circ \alpha} A(t) = I_{t_0, t}^{\alpha} A(t) = \frac{1}{\Gamma(\alpha)} \int_{t_0}^{t} \frac{A(\tau)}{(t - \tau)^{1 - \alpha}} d\tau$$

$$I_{t_0, t}^{(k+1) \circ \alpha} A(t) = I_{t_0, t}^{\alpha} \left(I_{t_0, t}^{k \circ \alpha} A(t) \right)$$

$$= \frac{1}{\Gamma(\alpha)} \int_{t_0}^{t} \frac{A(\tau) I_{t_0, \tau}^{k \circ \alpha} A(\tau)}{(t - \tau)^{1 - \alpha}} d\tau, \quad k \geq 1 \tag{21}$$

Let us consider now a fractional-order commensurate nonlinear chaotic system described by

$$D^\alpha x(t) = f(x(t), u(t), d(t))$$
$$y(t) = Cx(t) + Vd(t) \tag{22}$$

where $x(t) = [x_1(t) \quad x_2(t) \quad \ldots \quad x_n(t)]^{\mathrm{T}} \in \mathbb{R}^n$ is the n-dimensional state vector, $u(t) \in \mathbb{R}^m$ the input control vector, $y(t) \in \mathbb{R}^p$ the output vector and $d(t) \in \mathbb{R}^{n_d}$ the disturbance vector. Using the nonlinear sector transformation [43,44], an exact T–S representation for (22) is obtained as follows [41]

$$D^\alpha x(t) = \sum_{i=1}^{s} \mu_i(\xi) \left(A_i x(t) + B_i u(t) + W_i d(t)\right)$$
$$y(t) = Cx(t) + Vd(t) \tag{23}$$

where s denotes the number of linear models and the nonnegative functions $\mu_i(\xi)$ called the weighting functions or the membership functions satisfy the convex sum constraint formulated as

$$\sum_{i=1}^{s} \mu_i(\xi) = 1$$
$$\mu_i(\xi) \geq 0, \quad i = 1, 2, \ldots, s \tag{24}$$

These weighted functions depend on the variables $\xi(t) \in \mathbb{R}^q$ defined as the premise variables or the decision variables. We consider in this paper that the premise variables are available from measurements, i.e., $\xi(t)$ depends only on the outputs $y(t)$. In the most general second case, $\xi(t)$ depends on the unavailable state vector $x(t)$.

The main objective of the present paper is to propose an impulsive finite convergence time observer for the T–S fuzzy system (23). This will be the goal of the next section. First, we need some stability results that will be used to demonstrate the main results. Stability of uncertain T–S fuzzy fractional-order systems is investigated in [50] by using the linear matrix inequality (LMI) techniques. The following result is a particular case of those established in [50] when the uncertainties are absent. Indeed, using Lemmas 2 and 3, asymptotic stability of the following fractional-order T–S system

$$D^\alpha x(t) = \sum_{i=1}^{s} \mu_i(\xi) \left(A_i x(t)\right) \tag{25}$$

is stated in the two following theorems.

Theorem 2 *The fractional-order T–S system given by* (25) *with* $0 < \alpha < 1$ *is asymptotically stable if there*

exists a positive definite matrix $X > 0$ such that the following LMIs

$$A_i^{\mathrm{T}} X + X A_i < 0 \tag{26}$$

are satisfied for all $i = 1, 2, \ldots, s$.

Proof From Lemma 2 and by setting $P_{11} = P_{21} = X$ and $P_{12} = P_{22} = 0$, (25) is asymptotically stable if

$$\mathrm{Sym} \left(\Theta_{11} \otimes \left(\sum_{i=1}^{s} \mu_i(\xi) A_i^{\mathrm{T}} X \right) \right. $$
$$\left. + \Theta_{21} \otimes \left(\sum_{i=1}^{s} \mu_i(\xi) A_i X \right) \right) < 0$$

Using the following properties of the Kronecker product

$$A \otimes C + B \otimes C = (A + B) \otimes C$$
$$(A \otimes B)^{\mathrm{T}} = A^{\mathrm{T}} \otimes B^{\mathrm{T}}$$
$$(rA) \otimes B = r(A \otimes B), \forall r \in \mathbb{R} \tag{27}$$

and by the associativity property of the operator Sym, then the above stability condition is equivalent to

$$\mathrm{Sym} \left(2\Theta \otimes \sum_{i=1}^{s} \mu_i(\xi) A_i^{\mathrm{T}} X \right) < 0$$

where

$$\Theta = \begin{bmatrix} \sin(\theta) & 0 \\ 0 & \sin(\theta) \end{bmatrix}$$

and $\theta = \alpha \frac{\pi}{2}$. Then, it sufficient that the following condition

$$\sum_{i=1}^{s} \mu_i(\xi) \sin(\theta) \left(A_i^{\mathrm{T}} X + X A_i \right) < 0$$

is satisfied. Since $\sin(\theta) > 0$ for $0 < \alpha < 1$ and since the membership functions $\mu_i(\xi)$ are all nonnegative, it follows that the sufficient stability condition becomes

$$A_i^{\mathrm{T}} X + X A_i < 0, \quad i = 1, 2, \ldots, s$$

This completes the proof. $\qquad\square$

Similar result for the case $1 \leq \alpha < 2$ is established below.

Theorem 3 *The fractional-order T–S system given by* (25) *with* $1 \leq \alpha < 2$ *is asymptotically stable if there exists a real symmetric positive definite matrix* $X > 0$ *such that the following LMIs*

$$\begin{bmatrix} \left(A_i^{\mathrm{T}} X + X A_i\right) \sin(\tilde\theta) & \left(A_i^{\mathrm{T}} X - X A_i\right) \cos(\tilde\theta) \\ (*) & \left(A_i^{\mathrm{T}} X + X A_i\right) \sin(\tilde\theta) \end{bmatrix} < 0 \tag{28}$$

with $\tilde\theta = \pi - \alpha \frac{\pi}{2}$ *are satisfied for all* $i = 1, 2, \ldots, s$.

Proof From Lemma 3 and by setting $P = X$, (25) is asymptotically stable if there exists a real symmetric positive definite matrix $X > 0$, such that

$$
\left(\tilde{\Theta} \otimes \sum_{i=1}^{s} \mu_i(\xi) A_i^{\mathrm{T}} X \right)
$$
$$
+ \left(\tilde{\Theta} \otimes \sum_{i=1}^{s} \mu_i(\xi) A_i^{\mathrm{T}} X \right)^{\mathrm{T}} < 0, \quad i = 1, 2, \ldots, s
$$

where $\tilde{\Theta}$ is given by (15). Using properties (27) of the Kronecker product, it follows that the above inequality is equivalent to

$$
\sum_{i=1}^{s} \mu_i(\xi) \left(\tilde{\Theta} \otimes A_i^{\mathrm{T}} X + \tilde{\Theta}^{\mathrm{T}} \otimes X A_i \right) < 0, \quad i = 1, 2, \ldots, s
$$

Since the membership function $\mu_i(\xi)$, $i = 1, 2, \ldots, s$, is positive, a sufficient asymptotic stability condition is given by

$$
\tilde{\Theta} \otimes A_i^{\mathrm{T}} X + \tilde{\Theta}^{\mathrm{T}} \otimes X A_i < 0, \quad i = 1, 2, \ldots, s
$$

Substituting $\tilde{\Theta}$ by its expression given by (15) and expanding the Kronecker product, we conclude that the fractional-order T–S system (25), with $1 \leq \alpha < 2$, is asymptotically stable if LMIs (28) are satisfied. This completes the proof. □

Remark 2 Identical results for Theorems 2 and 3 are proposed in [50,55], concerning uncertain fractional-order systems (see, for example, Corollary 1 in [55]).

3 Main results

In this section, an impulsive state observer with a pre-defined convergence time is designed on the basis of the T–S fuzzy representation (23). The original idea was proposed for integer-order linear systems in [38] and then has been recently extended to fractional-order linear systems in [40]. In the first case, we consider the system without unknown input $d(t)$, and in the second case, we consider that the system is subject to the unknown input $d(t)$. In both cases, we assume that the premise variables $\xi(t)$ are available from measurement.

3.1 Case without unknown input

Let us rewrite the T–S fuzzy fractional-order system without unknown input as follows

$$
D^{\alpha} x(t) = \sum_{i=1}^{s} \mu_i(\xi) \left(A_i x(t) + B_i u(t) \right)
$$
$$
y(t) = C x(t) \tag{29}
$$

Let us consider the following assumption.

Assumption 1 The couples (A_i, C), $i = 1, 2, \ldots, s$ are observable.

Define updates time instants t_k such that $0 < t_1 < t_2 < \cdots < t_k < \cdots$, with $\lim_{k \to \infty} t_k = \infty$. Denotes by $t_k^+ = \lim_{h \to 0}(t_k + h)$ and $t_k^- = \lim_{h \to 0}(t_k - h)$ where $h \in \mathbb{R}_+$. For system (29), the T–S observer is described by

$$
D^{\alpha} z(t) = \sum_{i=1}^{s} \mu_i(\xi) \left(F_i z(t) \right.
$$
$$
\left. + G_i u(t) + L_i y(t) \right), \quad t \neq t_k
$$
$$
z(t_k^+) = K_k z(t_k^-), \quad t = t_k, \quad k = 1, 2, \ldots, \tag{30}
$$
$$
z(t_0) = M \hat{x}(t_0) = M \hat{x}_0
$$
$$
\hat{x}(t) = N z(t)
$$

with

$$
F_i = \begin{bmatrix} F_{i1} & 0_{n \times n} \\ 0_{n \times n} & F_{i2} \end{bmatrix}, \quad G_i = \begin{bmatrix} B_i \\ B_i \end{bmatrix} \tag{31}
$$

$$
L_i = \begin{bmatrix} L_{i1} \\ L_{i2} \end{bmatrix}, \quad M = \begin{bmatrix} I_n \\ I_n \end{bmatrix}, \quad N = \begin{bmatrix} I_n & 0_{n \times n} \end{bmatrix} \tag{32}
$$

The augmented state vector $z(t) \in \mathbb{R}^{2n}$ is partitioned as $z(t) = [z_1^{\mathrm{T}}(t) \ z_2^{\mathrm{T}}(t)]^{\mathrm{T}}$, respectively, with $z_1(t) \in \mathbb{R}^n$ and $z_2(t) \in \mathbb{R}^n$. $z(t_k^+)$ and $z(t_k^-)$ denote the right- and left-limit operators, respectively, defined as $z(t_k^+) = \lim_{h \to 0} z(t_k + h)$, $z(t_k^-) = \lim_{h \to 0} z(t_k - h)$ and by definition we take $z(t_k^-) = z(t_k)$. $L_{ij}, i = 1, 2, \ldots, s, j = 1, 2$, represent the classical Luenberger-type observer gains, i.e., with a linear output injection, while K_k, $k = 1, 2, \ldots$, represent the update gains with impulsive action. The time instants t_k, $k = 1, 2, \ldots$, of the observer state updates can be arbitrarily chosen. The design parameters of the T–S observer (30) include the matrices F_{ij}, G_i and the gains L_{ij} and K_k. These parameters are designed such that the T–S observer (30) converges in finite time $\delta = t_1 - t_0$ as stated by the following theorem.

Theorem 4 *Consider the fractional-order T–S system* (29) *with* $0 < \alpha < 1$ *and the corresponding T–S*

observer (30). *Let Assumption* 1 *be satisfied. If there exist symmetric positive definite matrices* $X_j > 0$ *and* Y_{ij} *such that the following LMI conditions*

$$
A_i^{\mathrm{T}} X_j + X_j A_i \\
- Y_{ij} C - C^{\mathrm{T}} Y_{ij}^{\mathrm{T}} < 0; \quad j = 1, 2; \quad i = 1, 2, \dots, s
$$
(33)

hold and if the update gains K_k *are given as follows*

$$
K_1 = M \left[I_n - \Phi_2(t_1, t_0) \Phi_1^{-1}(t_1, t_0) \right]^{-1} \\
\left[\Phi_2(t_1, t_0) \Phi_1^{-1}(t_1, t_0) \quad I_n \right] \\
K_k = I_{2n}, \quad k = 2, 3, \dots
$$
(34)

where $\Phi_j(t, t_0)$, $j = 1, 2$ *are solutions of the following fractional-order time-varying differential equations*

$$
D^\alpha \Phi_j(t, t_0) \\
= \sum_{i=1}^s \mu(\xi(t)) F_{ij} \Phi_j(t, t_0), \quad \Phi_j(t_0, t_0) = I_n, \quad j = 1, 2
$$
(35)

then the estimate $\hat{x}(t)$ *provided by the proposed impulsive T–S observer* (30) *with the following matrices*

$$
L_{ij} = X_j^{-1} Y_{ij}
$$
(36)
$$
F_{ij} = A_i - L_{ij} C
$$
(37)

converges to the true state $x(t)$ *in the predefined time* $\delta = t_1 - t_0$, *i.e.,* $e(t) = x(t) - \hat{x}(t) = 0$ *for all* $t \geq t_1$.

Proof Define the error $e_{zj} = x(t) - z_j(t)$, $j = 1, 2$. Let us write the fractional-order dynamical equation of e_{zj} over the interval time $[t_0 \quad t_1]$. In this time interval, according to (31) and (32), we have

$$
D^\alpha z_j(t) = \sum_{i=1}^s \mu_i(\xi) \left(F_{ij} z_j(t) + B_i u(t) + L_{ij} y(t) \right)
$$
(38)

Then,

$$
D^\alpha e_{zj}(t) = \sum_{i=1}^s \mu_i(\xi) \left(A_i x(t) - F_{ij} z_j(t) - L_{ij} C x(t) \right)
$$
(39)

Since $F_{ij} = A_i - L_{ij} C$, then

$$
D^\alpha e_{zj}(t) = \sum_{i=1}^s \mu_i(\xi) \left(F_{ij} e_{zj}(t) \right)
$$
(40)

The observer gains L_{ij} are designed so that the estimation error dynamic equation (40) is asymptotically

stable. Thanks to Theorem 2, the asymptotic stability is guaranteed if there exists two matrices $X_j > 0$, $j = 1, 2$ such that the LMIs

$$
F_{ij}^{\mathrm{T}} X_j + X_j F_{ij} < 0, \quad i = 1, 2, \dots, s; \quad j = 1, 2
$$
(41)

are satisfied. This is always possible by Assumption 1. By introducing the variables (36) and (37) in (41), we can check that the LMIs (41) are equivalent to those of (33). Then, for any initial value $e_{zj0} = e_{zj}(t_0)$, the error $e_{zj}(t)$ evolves in convergent manner. Moreover, we have

$$
e_{zj}(t) = \Phi_j(t, t_0) e_{zj0}
$$
(42)

where $\Phi_j(t, t_0)$ is the state transition matrix, solution of (35). Consider now the first update instant t_1. At this time, we have from (42)

$$
z_j(t_1) = x(t_1) - \Phi_j(t_1, t_0)(x_0 - \hat{x}_0)
$$
(43)

At $t = t_1^+$, the evolution of $z_j(t)$, $j = 1, 2$ is forced as

$$
z(t_1^+) = K_1 z(t_1^-) = K_1 z(t_1)
$$
(44)

Substituting (43) in (44) yields to

$$
\begin{bmatrix} z_1(t_1^+) \\ z_2(t_1^+) \end{bmatrix} = K_1 M x(t_1) \\
- K_1 \begin{bmatrix} \Phi_1(t_1, t_0) & 0_{n \times n} \\ 0_{n \times n} & \Phi_1(t_1, t_0) \end{bmatrix} M(x_0 - \hat{x}_0)
$$
(45)

Substituting (34) in (45), one can easily check that

$$
z_1(t_1^+) = z_2(t_1^+) = x(t_1)
$$
(46)

This amounts to saying that after the jump instant t_1, the Luenberger-type observer (30) is initialized by the exact value of the true state $x(t_1)$. It follows that $\hat{x}(t) = x(t)$ for all $t \geq t_1$. Then the observer exactly converges in finite time $\delta = t_1 - t_0$. This completes the proof. □

Remark 3 The design problem of the proposed observer focuses on solving the LMIs (33). Numerical tools are available in the literature such as the YALMIP toolbox in MATLAB [63]. Moreover, we must avoid the singularity that can appear in the calculation of the gain K_1 for $t_1 > 0$. For this purpose, the two transition matrices $\Phi_1(t, t_0)$ and $\Phi_2(t, t_0)$ should be different. To achieve this, the LMIs (33) may be solved by pole placement. It is sufficient to locate the poles in a LMI region of the complex left half plane [64].

Let $\Omega_j(\rho_j)$, $\rho_j > 0$, $j = 1, 2$ be a subregion of the complex left half plane limited, at the right side, by a vertical straight of coordinate in the real axis equal to $-\rho_j$ with $\rho_1 \neq \rho_2$. The LMIs with the prescribed region $\Omega_j(\rho_j)$ are expressed as follows [64]

$$A_i^{\mathrm{T}} X_j + X_j A_i - Y_{ij} C - C^{\mathrm{T}} Y_{ij}^{\mathrm{T}} + 2\rho_j X_j < 0; \ j = 1, 2; \quad i = 1, 2, \ldots, s \quad (47)$$

The fact that $\rho_1 \neq \rho_2$ avoids the singularity of K_1. The state transition matrices $\Phi_1(t, t_0)$ and $\Phi_2(t, t_0)$ are numerically determined by solving the fractional-order differential equation (35) using, for example, the numerical Grunwald–Letnikov formulae of the fractional-order derivative defined as follows. The Grunwald–Letnikov derivative of a function $f(t)$ is given by [58]

$$\begin{aligned} &{}_{t_0}^{\mathrm{GL}} D^{\alpha} f(t) \mid_{t=kh} \\ &\approx \frac{1}{h^{\alpha}} \sum_{j=0}^{j=[(t-t_0)/h]} (-1)^j \binom{\alpha}{j} \cdot f(kh - jh) \end{aligned}$$

where the binomial term is given by

$$\binom{\alpha}{j} \cdot = \frac{\alpha(\alpha - 1)(\alpha - 2) \ldots (\alpha - j + 1)}{j!}$$

h is the sampling step and $[s]$ denotes the integer part of s.

Remark 4 Assumption 1 of observability of local subsystems (A_i, C), $i = 1, 2, \ldots, s$ is necessary to the existence of the observer gains L_{ij}, $i = 1, 2, \ldots, s$, $j = 1, 2$ [65].

Next, the result of Theorem 4 is extended to the case of $1 \leq \alpha < 2$. The same structure (30) is kept. Only the conditions of convergence of the estimation error formulated by relation (41) are modified. This leads to the corollary below.

Corollary 1 *Consider the fractional-order T–S system* (29) *with* $1 \leq \alpha < 2$ *and the corresponding T–S observer* (30). *Let Assumption 1 be satisfied. If there exist matrices* $X_j > 0$, Y_{ij} *such that the following LMI conditions*

$$\begin{bmatrix} \mathscr{F}_{ij} \sin(\tilde{\theta}) & \bar{\mathscr{F}}_{ij} \cos(\tilde{\theta}) \\ \bar{\mathscr{F}}_{ij} \cos(\tilde{\theta}) & \mathscr{F}_{ij} \sin(\tilde{\theta}) \end{bmatrix} \\ < 0, \quad j = 1, 2; \quad i = 1, 2, \ldots, s \quad (48)$$

with

$$\mathscr{F}_{ij} = A_i^{\mathrm{T}} X_j + X_j A_i - Y_{ij} C - C^{\mathrm{T}} Y_{ij}^{\mathrm{T}} \quad (49)$$

$$\bar{\mathscr{F}}_{ij} = A_i^{\mathrm{T}} X_j - X_j A_i + Y_{ij} C - C^{\mathrm{T}} Y_{ij}^{\mathrm{T}} \quad (50)$$

are satisfied, then the estimate state $\hat{x}(t)$ *provided by the impulsive observer* (30) *with* $1 \leq \alpha < 2$ *and with the design parameters are given, as in Theorem 4, by relations* (34)–(37)*, converges to the true state* $x(t)$ *in the predefined time* $\delta = t_1 - t_0$*, i.e.,* $e(t) = x(t) - \hat{x}(t) = 0$ *for all* $t \geq t_1$*.*

Proof According to same developments given in the proof of Theorem 4, the dynamic of the estimation error $e_{zj} = x(t) - z_j(t)$ $j = 1, 2$ is governed by Equation (40). Thanks to Theorem 3, the estimation error e_{zj} is asymptotically stable if there exist real symmetric positive definite matrices $X_j > 0$, $j = 1, 2$ such that

$$\begin{bmatrix} \left(F_{ij}^{\mathrm{T}} X_j + X_j F_{ij}\right) \sin(\tilde{\theta}) & \left(F_{ij}^{\mathrm{T}} X_j - X_j F_{ij}\right) \cos(\tilde{\theta}) \\ (*) & \left(F_{ij}^{\mathrm{T}} X_j + X_j F_{ij}\right) \sin(\tilde{\theta}) \end{bmatrix} \\ < 0, \quad j = 1, 2; \quad i = 1, 2, \ldots s \quad (51)$$

where $\tilde{\theta} = \pi - \alpha \frac{\pi}{2}$. Using relations (36) and (37), it easy to check that the above LMIs are equivalent to LMIs given by (48) with (49) and (50). The rest of the proof is similar to the proof of Theorem 4. □

3.2 Case with unknown input

Now, we consider that the fractional-order system is subject to the unknown input vector $d(t)$ and is described by the T–S model (23). Consider the following assumptions.

Assumption 2 The disturbance vector $d(t)$ is unknown and bounded.

Assumption 3 The matrices W_i, $i = 1, 2, \ldots, s$, V and C are full rank, i.e., $\mathrm{rank}(W_i) = rank(V) = n_d$, $i = 1, 2, \ldots, s$ and $\mathrm{rank}(C) = p$.

The proposed impulsive observer with predetermined finite-time convergence is given by

$$\begin{aligned} D^{\alpha} \eta(t) &= \sum_{i=1}^{s} \mu_i(\xi)(F_i \eta(t) \\ &\quad + G_i u(t) + L_i y(t)), \quad t \neq t_k \\ z(t) &= \eta(t) - E y(t), \quad t \neq t_k \\ z(t_k^+) &= K_k z(t_k^-), \eta(t_k^+) \end{aligned}$$

$$= z(t_k^+) + E y(t_k)^+, \quad t = t_k, \quad k = 1, 2, \ldots,$$

$$z(t_0) = M \hat{x}(t_0) = M \hat{x}_0$$

$$\hat{x}(t) = N z(t) \tag{52}$$

$$L_i = \begin{bmatrix} L_{i1} \\ L_{i2} \end{bmatrix}, \quad E = \begin{bmatrix} E_1 \\ E_2 \end{bmatrix}, \quad G_i = \begin{bmatrix} G_{i1} \\ G_{i2} \end{bmatrix} \tag{53}$$

The matrices M and N are given in relation (32). The augmented state vectors $\eta(t) \in \mathbb{R}^{2n}$ and $z(t) \in \mathbb{R}^{2n}$ are partitioned as $\eta(t) = [\eta_1^T(t) \quad \eta_2^T(t)]^T$ and $z(t) = [z_1^T(t) \quad z_2^T(t)]^T$, respectively, with $\eta_1(t) \in \mathbb{R}^n, \eta_2(t) \in \mathbb{R}^n, z_1(t) \in \mathbb{R}^n$ and $z_2(t) \in \mathbb{R}^n$. The following theorem states the result on the finite-time convergence of the proposed impulsive T–S fuzzy observer (52).

Theorem 5 *Consider the fractional-order T–S fuzzy system* (23) *with* $0 < \alpha < 1$ *and the corresponding T–S observer* (52). *Let Assumptions 2–3 be satisfied. If, there exist matrices* $X_j > 0$, S_j *and* Y_{ij}, $i = 1, 2, \ldots, s$, $j = 1, 2$ *such that the following LMI conditions*

$$A_i^T X_j + X_j A_i + A_i^T C^T S_j^T$$
$$+ S_j C A_i - C^T Y_{ij}^T - Y_{ij} C < 0 \tag{54}$$

hold with the equality constraints

$$\left(X_j + S_j C \right) W_i = Y_{ij} V \tag{55}$$

$$S_j V = 0 \tag{56}$$

and if the update gains K_k *are designed as*

$$K_1 = M \left[I_n - \Phi_2(t_1, t_0) \Phi_1^{-1}(t_1, t_0) \right]^{-1}$$
$$\left[\Phi_2(t_1, t_0) \Phi_1^{-1}(t_1, t_0) \quad I_n \right]$$
$$K_k = I_{2n}, \quad k = 2, 3, \ldots \tag{57}$$

where $\Phi_j(t, t_0)$, $j = 1, 2$ *are solutions of the fractional-order differential equations*

$$D^\alpha \Phi_j(t, t_0) = \sum_{i=1}^{s} \mu(\xi(t)) F_{ij} \Phi_j(t, t_0),$$
$$\Phi_j(t_0, t_0) = I_n, \quad j = 1, 2 \tag{58}$$

then, for any unknown bounded input $d(t)$, *the state estimate vector* $\hat{x}(t)$ *provided by the impulse functional T–S observer* (52) *with the following matrices*

$$E_j = X_j^{-1} S_j$$

$$G_{ij} = \left(I_n + X_j^{-1} S_j C \right) B_i$$

$$F_{ij} = \left(I_n + X_j^{-1} S_j C \right) A_i - X_j^{-1} Y_{ij} C$$

$$L_{ij} = X_j^{-1} Y_{ij} - F_{ij} E_j \tag{59}$$

converges to the true state vector $x(t)$ *in the predefined time* $\delta = t_1 - t_0$, *i.e.,*

$$e(t) = x(t) - \hat{x}(t) = 0, \quad \forall t \geq t_1 \tag{60}$$

Proof Define the estimation error $e_{zj}(t) = x(t) - z_j(t)$, $j = 1, 2$. Then

$$D^\alpha e_{zj} = D^\alpha x(t) - D^\alpha z_j(t)$$
$$= D^\alpha x(t) - D^\alpha \eta_j(t) + E_j C D^\alpha x(t) + E_j V D^\alpha d(t) \tag{61}$$

Taking the fact that

$$D^\alpha \eta_j(t) = \sum_{i=1}^{s} \mu_i(\xi)(F_{ij} \eta_j(t)$$
$$+ G_{ij} u(t) + L_{ij} C x(t) + L_{ij} V d(t)) \tag{62}$$

and using the convexity property of the membership function $\mu_i(\xi)$, we obtain

$$D^\alpha e_{zj}(t) = \sum_{i=1}^{s} \mu_i(\xi) \left\{ F_{ij} e_{zj}(t) \right.$$
$$+ (P_j A_i - F_{ij} A_i - L_{ij} C) x(t)$$
$$+ (P_j B_i - G_{ij}) u(t)$$
$$\left. + (P_j W_i - E_j V - L_{ij} V) d(t) + E_j V d(t) \right\} \tag{63}$$

where

$$P_j = (I_n + E_j C) \tag{64}$$

If the observer matrices F_{ij}, G_{ij}, L_{ij} and E_j are designed such that the relations

$$P_j A_i - F_{ij} P_j - L_{ij} C = 0$$
$$G_{ij} = P_j B_i$$
$$P_j W_i - F_{ij} E_j V - L_{ij} V = 0$$
$$E_j V = 0 \tag{65}$$

are satisfied for $i = 1, 2, \ldots, s$ and $j = 1, 2$, the estimation error e_{zj} obeys the following equation

$$D^\alpha e_{zj}(t) = \sum_{i=1}^{s} \mu_i(\xi) \left(F_{ij} e_{zj}(t) \right) \tag{66}$$

According to Theorem 2, the above system is asymptotically stable if there exist symmetric positive definite matrices X_j, $j = 1, 2$, such that the following LMIs

$$F_{ij}^T X_j + X_j F_{ij} < 0; \quad i = 1, 2, \ldots, s; \quad j = 1, 2 \tag{67}$$

hold. Introduce the following change of variables

$$E_j = X_j^{-1} S_j$$
$$L_{ij} = X_j^{-1} Y_{ij} - F_{ij} E_j \tag{68}$$

Then, we can show, after some straightforward algebraic calculations, that relations (65) are equivalent to

$$F_{ij} = (I_n + X_j^{-1} S_j C) A_i - X_j S_j C$$
$$G_{ij} = (I_n + X_j^{-1} S_j) B_i$$
$$(I_n + X_j^{-1} S_j) W_i - Y_{ij} V = 0$$
$$S_j V = 0 \tag{69}$$

and the LMIs (67) are equivalent to the LMIs (54). Now, if the above conditions are satisfied, then at the time t_1, we have exactly the same situation as in Theorem 4. The rest of the proof is identical to Theorem 4. Therefore, the injection of the update gain K_1 forces the state $\hat{x}(t_1)$ to be equal to the true state $x(t_1)$. We conclude then that $\hat{x}(t) = x(t)$ for all $t \geq t_1$. This completes the proof. □

Remark 5 Assumption 3 is necessary for the possible existence of the proposed observer. Indeed, the existence of this observer depends on the feasibility of the LMIs (54) and also the equality constraints (55), (56). These equalities are satisfied under Assumption 3.

Remark 6 Assumption 2 allows us to avoid the divergence of the solutions of the system subject to an unbounded input. In addition, in the application to chaotic synchronization, the amplitude of the input $d(t)$ must be small enough to preserve the chaotic behavior of the system.

Remark 7 As in the case of the observer without unknown input developed above, the design of the unknown input observer (52) requires that the update gain K_1 exists. Therefore, the two transition matrices $\Phi_1(t, t_0)$ and $\Phi_2(t, t_0)$ should be different. For this purpose, consider the LMI regions $\tilde{\Omega}_J(\rho_J, \sigma_J)$, $j = 1, 2$ defined in the complex plan as the intersection between the circle of center $(0, 0)$ and of radius σ_j and the left half plane limited by a vertical straight line of abscissa equal to $-\rho_j$, $\rho_j > 0$. The LMI conditions (54) with the above regions are equivalent to

$$\begin{bmatrix} -\sigma_j X_j & X_j A_i + S_j C A_i - Y_{ij} C \\ (*) & -\sigma_j X_j \end{bmatrix}$$
$$< 0, \quad j = 1, 2 \tag{70}$$
$$A_i^T X_j + X_j A_i + A_i^T C^T S_j^T$$

$$+ S_j C A_i - C^T Y_{ij} - Y_{ij} C + 2\rho_j < 0, \quad j = 1, 2 \tag{71}$$

with the equality constraints (55) and (56). LMIs (70), (71) can be solved with the YALMIP/MATLAB package.

The extension of Theorem 5 results to the case of $1 \leq \alpha < 2$ is derived in the following corollary.

Corollary 2 *In Theorem* 5, *if* $1 \leq \alpha < 2$ *and if the LMI* (54) *is replaced by the following LMIs*

$$\begin{bmatrix} \mathscr{H}_{ij} \sin(\tilde{\theta}) & \bar{\mathscr{H}}_{ij} \cos(\tilde{\theta}) \\ (*) & \mathscr{H}_{ij} \sin(\tilde{\theta}) \end{bmatrix} < 0,$$
$$j = 1, 2; \quad i = 1, 2, \ldots, s \tag{72}$$

with

$$\mathscr{H}_{ij} = A_i^T X_j + X_j A_i - A_i^T C^T S_j^T$$
$$+ S_j C A_i - C^T Y_{ij}^T - Y_{ij} C \tag{73}$$
$$\bar{\mathscr{H}}_{ij} = A_i^T X_j - X_j A_i - A_i^T C^T S_j^T$$
$$- S_j C A_i - C^T Y_{ij}^T + Y_{ij} C \tag{74}$$

and $\tilde{\theta} = \pi - \alpha \frac{\pi}{2}$, *then the estimate state* $\hat{x}(t)$ *provided by the impulsive functional T–S observer* (52), (53) *with relations* (54)–(59) *exactly converges to the true state* $x(t)$ *in the predefined time* $\delta = t_1 - t_0$.

Proof The proof is similar to that of Theorem 5. Only conditions of convergence of the error $e_{zj}(t)$, $j = 1, 2$ governed by Eq. (66) are modified. Indeed, for $1 \leq \alpha < 2$, according to Theorem 4, the estimation error dynamic equation (66) is asymptotically stable, if there exist two symmetric positive definite matrices X_j, $j = 1, 2$ such that the following LMIs

$$\begin{bmatrix} \left(F_{ij}^T X_j + X_j F_{ij}\right) \sin(\tilde{\theta}) & \left(F_{ij}^T X_j - X_j F_{ij}\right) \cos(\tilde{\theta}) \\ (*) & \left(F_{ij}^T X_j + X_j F_{ij}\right) \sin(\tilde{\theta}) \end{bmatrix} < 0,$$
$$j = 1, 2; \quad i = 1, 2, \ldots s \tag{75}$$

are satisfied. Introducing the change of variables (69), it easy to check that the LMIs (75) is equivalent to the LMIs (72) with (73) and (74). The rest of the proof follows from the proof of Theorem 5. □

4 Numerical application to synchronization of fractional-order chaotic systems

This section is dedicated to illustrate the efficiency of proposed impulsive observers to fractional-order

chaotic synchronization. Consider the fractional-order Lorenz chaotic system with commensurate derivative orders described by [9]

$$D^\alpha x_1(t) = -ax_1(t) + ax_2(t)$$
$$D^\alpha x_2(t) = cx_1(t) - x_2(t) - x_1(t)x_3(t)$$
$$D^\alpha x_3(t) = x_1(t)x_2(t) - bx_3(t) \quad (76)$$

It has been shown that the system exhibits a chaotic behavior with the following values of the system parameters $a = 10$; $c = 28$, $b = 8/3$ and $\alpha > 0.9941$ [9]. Hereafter, the fractional derivative order is taken as $\alpha = 0.995$. Suppose that $x_1(t) \in [-30 \quad +30]$. Then, we can write

$$x_1(t) = \mu_1(x_1)X_{1\min} + \mu_2(x_1)X_{1\max} \quad (77)$$

where $X_{1\min} = -30$ and $X_{1\max} = -X_{1\min} = 30$. The membership functions are given by

$$\mu_1(x_1) = \frac{X_{1\max} - x_1}{2X_{1\max}}; \quad \mu_2(x_1) = \frac{X_{1\max} + x_1}{2X_{1\max}}$$
$$\mu_1(x_1) + \mu_2(x_1) = 1 \quad (78)$$

with $\mu_1(x_1) > 0$ and $\mu_2(x_1) > 0$. Then the fractional-order chaotic Lorenz system can be exactly represented by the following T–S model

$$D^\alpha x(t) = \mu_1(x_1)A_1 x(t) + \mu_2(x_1)A_2 x(t) \quad (79)$$

with

$$A_1 = \begin{bmatrix} -10 & 10 & 0 \\ 28 & -1 & 30 \\ 0 & -30 & -\frac{8}{3} \end{bmatrix}, A_2 = \begin{bmatrix} -10 & 10 & 0 \\ 28 & -1 & -30 \\ 0 & 30 & -\frac{8}{3} \end{bmatrix} \quad (80)$$

Note that in the sequel, for this example, we consider that $B_1 = B_2 = [0 \quad 0 \quad 0]^T$. All simulations are performed by using the Grunwald–Letnikov formula of the fractional-order derivative (see Remark 3) with a step calculation equal to $h = 0.001$. The state variable trajectories for both original nonlinear system and its T–S fuzzy representation are provided in Fig. 1. As can be seen, the trajectories for the two systems are strictly the same for the three state variables. Curves are practically confused. This is also illustrated in Fig. 2 where error curves are plotted. This confirms that the T–S representation of the nonlinear system is exact. We can also observe this fact in Fig. 3 which plots strange attractors for the original system (Fig. 3a in $(x_1 - x_2)$-plan and Fig. 3c in $(x_1 - x_3)$-plan) and for the corresponding T–S representation [Fig. 3b in $(x_1 - x_2)$-plan and Fig. 3d in $(x_1 - x_3)$-plan]. Strange attractors are correctly reproduced with the T–S model.

4.1 Observer without unknown input

The observer design problem given by (30) consists on resolving the LMIs (47). The output equation is taken as

$$y(t) = Cx(t) = \begin{bmatrix} 1 & 0 & 0 \\ 0 & 1 & 0 \end{bmatrix} x(t) \quad (81)$$

We can check that (A_1, C) and (A_2, C) are observable. Then Assumption 1 used in Theorem 4 is well satisfied. The decision variable x_1 is measurable since $y_1 = x_1$

Fig. 1 State variable trajectories **a** x_1, **b** x_2, **c** x_3 for the original nonlinear system (in black color) and for the T–S model (in red color). (Color figure online)
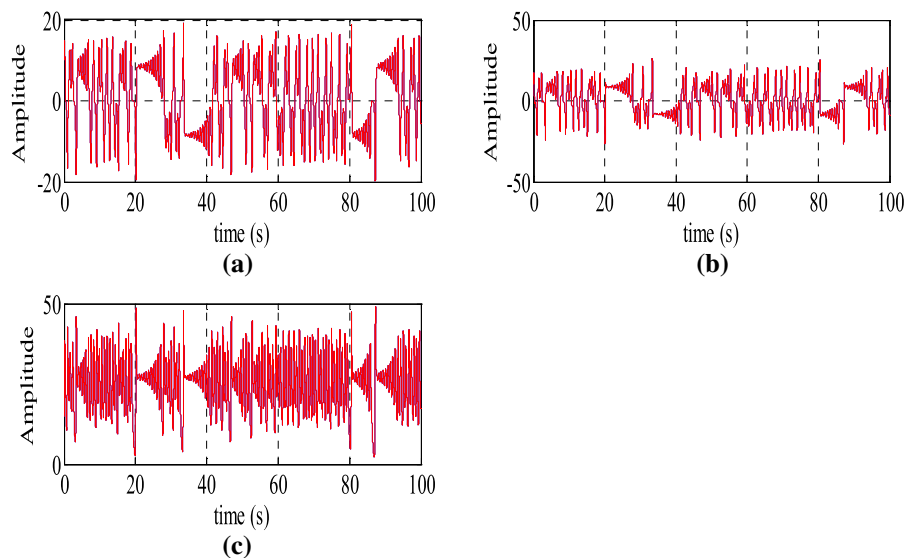
Fig. 2 Errors trajectories between the original system and the T–S model: **a** first state variable, **b** second state variable, **c** third state variable
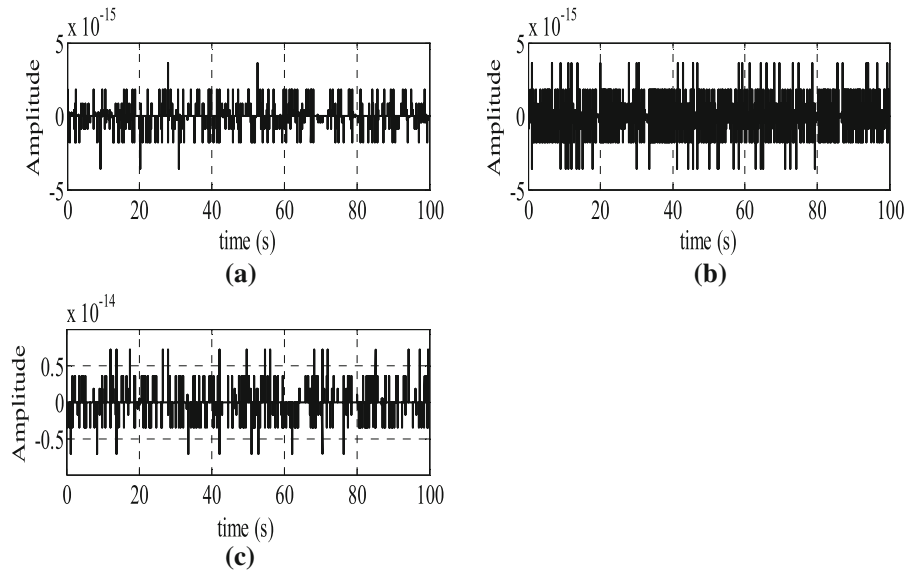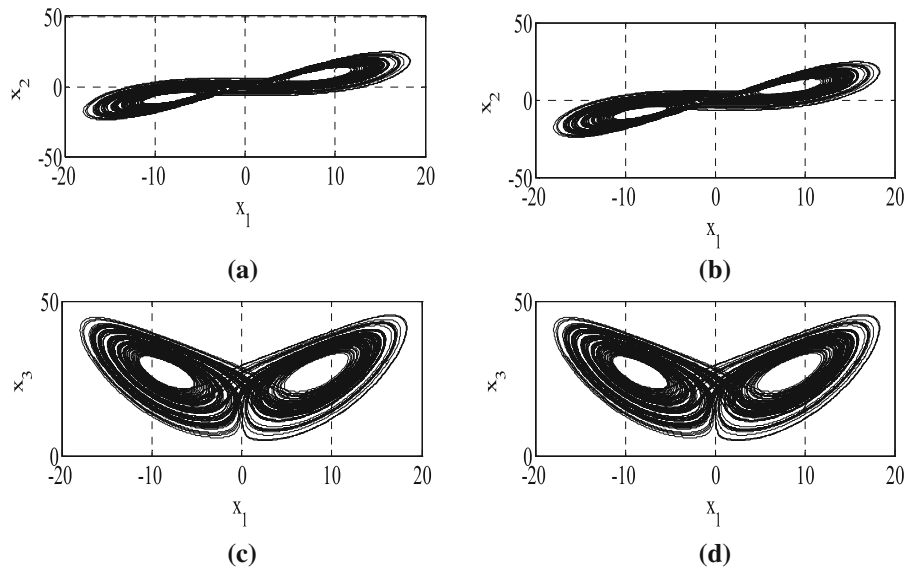

(a)

(b)

(c)

Fig. 3 Strange attractor in $(x_1 - x_2)$-plan **a** for original nonlinear system and **b** for T–S model. Strange attractor in $(x_1 - x_3)$-plan, **c** for original nonlinear system and **d** for T–S model

(a)

(b)

(c)

(d)

Using the YALMIP/MATLAB toolbox, we find that the linear matrix inequalities are feasible for $j = 1, 2$. The two transition matrices Φ_1 and Φ_2 should be different to avoid the singularity in the calculation of the update gain K_1. So, the LMIs are solved for $j = 1$ and $j = 2$ by using the pole placement strategy as discussed in Remark 3. The solutions X_1 and X_2 for $\rho_1 = 0.5$ and $\rho_2 = 0.7$ are given by

$$X_1 = \begin{bmatrix} 0.6794 & 0.0000 & 0.0000 \\ 0.0000 & 0.6794 & -0.0000 \\ 0.0000 & -0.0000 & 2.5723 \end{bmatrix},$$

$$X_2 = \begin{bmatrix} 0.6588 & 0.0000 & 0.0000 \\ 0.0000 & 0.6588 & 0.0000 \\ 0.0000 & 0.0000 & 2.2993 \end{bmatrix} \tag{82}$$

and the observer gains K_1, L_{ij}, $i = 1, 2$, $j = 1, 2$ are given as

$$L_{11} = \begin{bmatrix} -9.3301 & -12.5026 \\ 50.5026 & -0.3301 \\ 0.0000 & -83.5799 \end{bmatrix}, \quad L_{12} = \begin{bmatrix} -9.3301 & 11.8311 \\ 26.1689 & -0.3301 \\ -0.0000 & 83.5799 \end{bmatrix} \tag{83}$$

$$L_{21} = \begin{bmatrix} -9.2694 & -11.5447 \\ 49.5447 & -0.2694 \\ 0.0000 & -74.7102 \end{bmatrix}, \quad L_{22} = \begin{bmatrix} -9.2694 & 12.0491 \\ 25.9509 & -0.2694 \\ -0.0000 & 74.7102 \end{bmatrix} \tag{84}$$

$$K_1 = \begin{bmatrix} 12.6463 & 31.2072 & 0.0568 & -11.6463 & -31.2072 & -0.0568 \\ 29.4517 & 74.7156 & 3.8480 & -29.4517 & -73.7156 & -3.8480 \\ -10.4505 & -35.1791 & -1.2752 & 10.4505 & 35.1791 & 2.2752 \\ 12.6463 & 31.2072 & 0.0568 & -11.6463 & -31.2072 & -0.0568 \\ 29.4517 & 74.7156 & 3.8480 & -29.4517 & -73.7156 & -3.8480 \\ -10.4505 & -35.1791 & -1.2752 & 10.4505 & 35.1791 & 2.2752 \end{bmatrix} \tag{85}$$

The initial conditions are taken as $x_0 = [6 \ 5 \ 1]^T$ and $t_0 = 0$, while those of the observer are fixed to zero. Figures 4, 5 and 6 plot the trajectories of the true state variables $x_i(t)$ and their corresponding estimates $\hat{x}_i(t)$, $i = 1, 2, 3$, for $\delta = t_1 = 0.5s$, and in Fig. 7 are reported the trajectories of the estimation errors $e_i(t) = x_i(t) - \hat{x}_i(t)$, $i = 1, 2, 3$. As can be depicted from these figures, the estimated state variables converge exactly toward the true state variables in the predetermined time t_1, i.e., for all $t \geq t_1$, we have $\hat{x}_i(t) = x_i(t)$. In the zoomed parts of these figures, the impulsive behavior of the proposed observer is showed at the time t_1. This impulsive behavior corresponds to the abrupt update of the observer state, $z(t_1^+) = K_1 z(t_1^-)$ with K_1 given by (34). Thanks to

the judicious choice of the gain K_1, the estimated state provided by the proposed observer becomes immediately equal to the true state. Meanwhile, the proposed observer allows to obtain exact state observation after the predefined time t_1. Theoretically, the proposed observer is able to achieve instantaneous and exact synchronization immediately after t_1. However, some distortion with relatively small estimation error for $t > t_1$ may occur (Fig 7b) due to the discretization process in the numerical simulation and the use of the Grunwald–Letnikov formula as approximation of the fractional-order derivative significantly depending of the sampling time.

In order to highlight the performance of the proposed observer, we compare it to the sliding mode observer

Fig. 4 State variable x_1 (in black color) and its estimate $\hat{x}_1(t)$ (in red color) resulting from the proposed observer for $\delta = 0.5s$. (Color figure online)
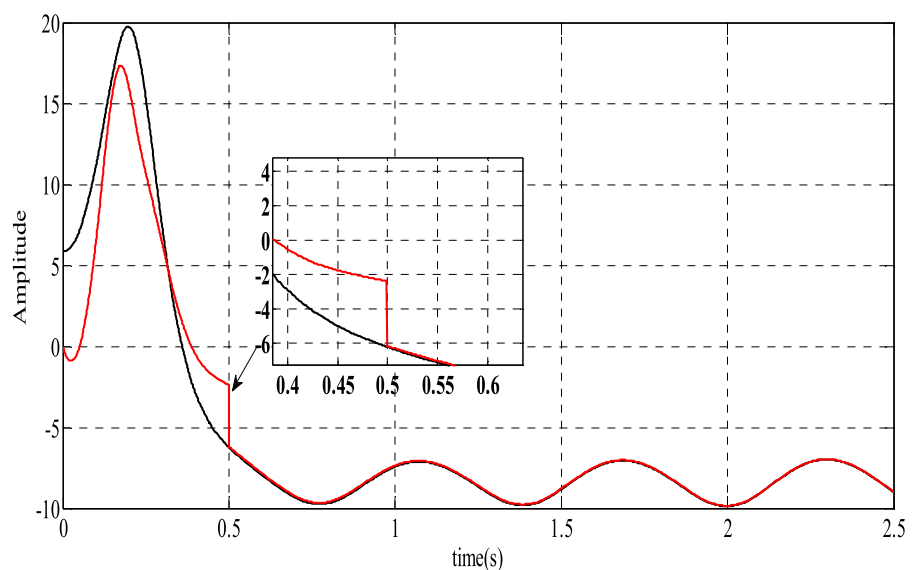
Fig. 5 State variable x_2 (in black color) and its estimate $\hat{x}_2(t)$ (in red color) resulting from the proposed observer for $\delta = 0.5s$. (Color figure online)
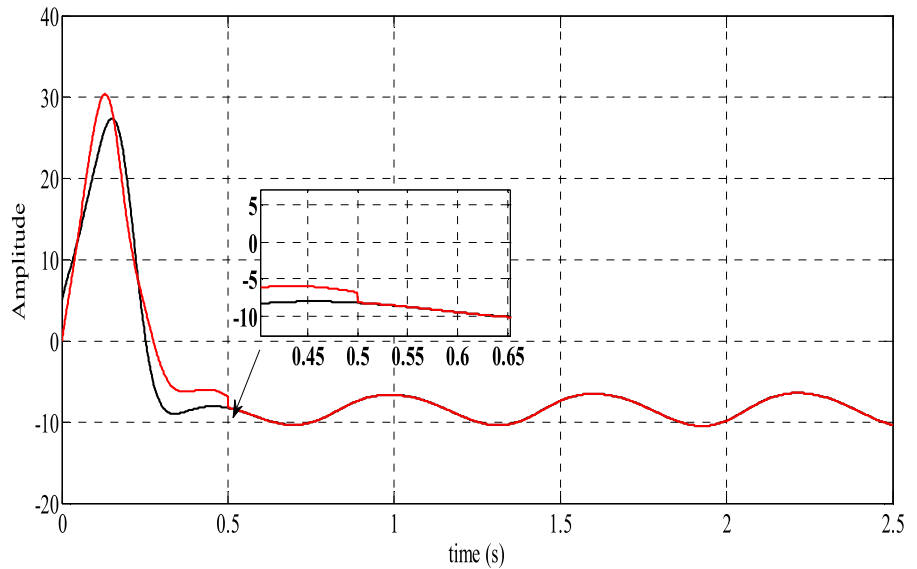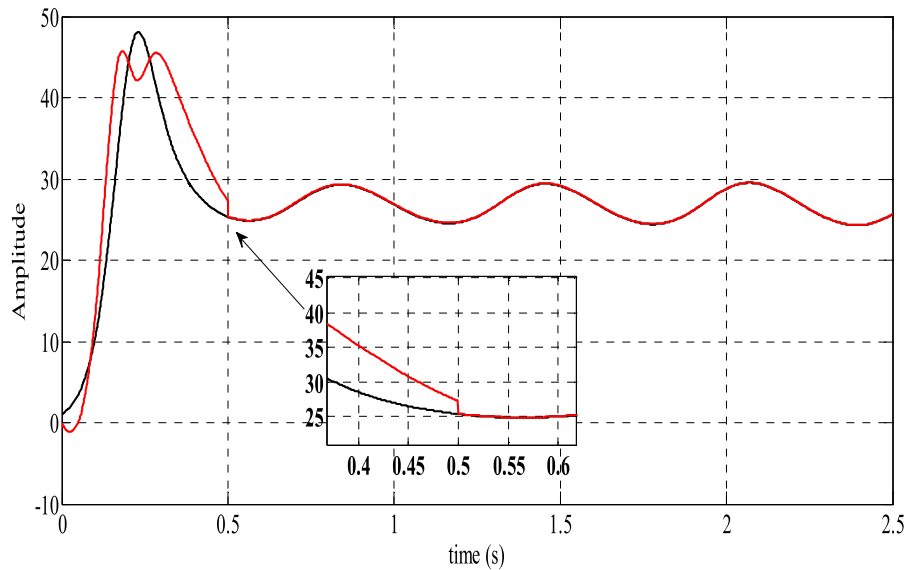

Fig. 6 State variable x_3 (in black color) and its estimate $\hat{x}_3(t)$ (in red color) resulting from the proposed observer for $\delta = 0.5s$. (Color figure online)

recognized as the most popular finite convergence time observer. A step-by-step sliding mode observer for the fractional-order Lorenz chaotic system (76) with the single output $y_1(t) = x_1(t)$ is described by the following equations

$$D^\alpha \hat{x}_{1mg}(t) = -ay_1(t) + a\hat{x}_{2mg}(t) + k_1 \text{sign}(\tilde{e}_1)$$
$$D^\alpha \hat{x}_{2mg}(t) = cy_1(t) - \tilde{x}_{2mg}(t) - y_1(t)\hat{x}_{3mg}(t)$$
$$+ E_1 k_2 sign(\tilde{e}_2)$$
$$D^\alpha \hat{x}_{3mg}(t) = y_1(t)\tilde{x}_{2mg}(t) - b\tilde{x}_3(t)E_2 k_3 \text{sign}(\tilde{e}_3)$$
$$\tilde{x}_{2mg} = \hat{x}_{2mg} + \frac{1}{a} + E1 k_1 \text{sign}(\tilde{e}_1)$$

$$\tilde{x}_{3mg} = \hat{x}_{3mg} - \frac{1}{y_1 + \varsigma} + E2 k_2 \text{sign}(\tilde{e}_2) \quad (86)$$

where $\hat{x}_{img}, i = 1, 2, 3$, denote the estimates of the state variables and $\tilde{e}_i(t) = \tilde{x}_i(t) - \hat{x}_i(t), i = 1, 2, 3$, are the intermediate estimation errors with $\tilde{x}_1(t) = x_1(t)$ by construction. The standard sign function is defined as follows.

$$\text{sign}(e) = \begin{cases} 1 & \text{if } e > 0 \\ 0 & \text{if } e = 0 \\ -1 & \text{if } e < 0 \end{cases}$$

$\varsigma = 0.0001$ denotes a small constant added in order to avoid division by zero. The estimation errors are

Fig. 7 Estimation errors for
$\delta = 0.5s$. **a**
$e_1(t) = x_1(t) - \hat{x}_1(t)$, **b**
$e_2(t) = x_2(t) - \hat{x}_2(t)$, **c**
$e_3(t) = x_3(t) - \hat{x}_3(t)$

(a)

(b)

(c)
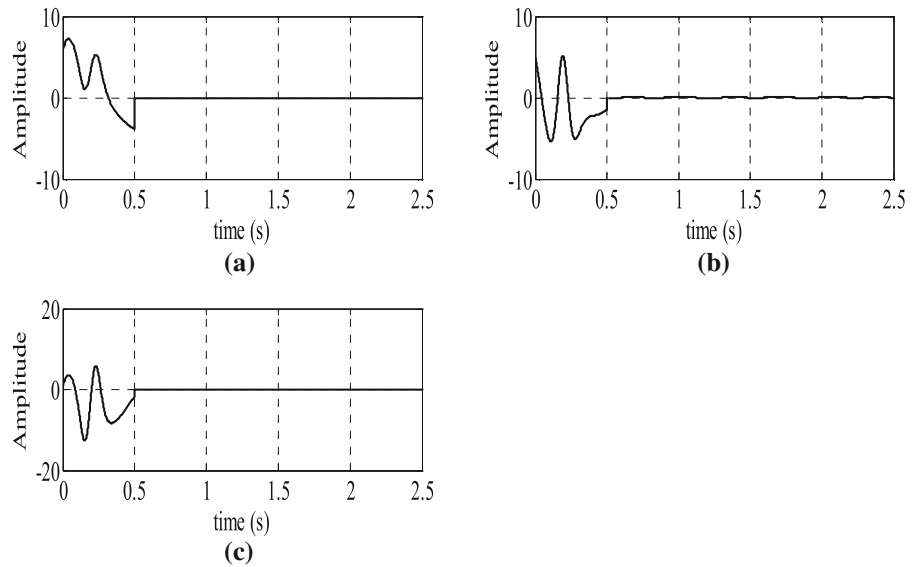
Fig. 8 State variable x_1 (in
black color) and its estimate
$\hat{x}_{1\mathrm{mg}}(t)$ (in red color)
resulting from the sliding
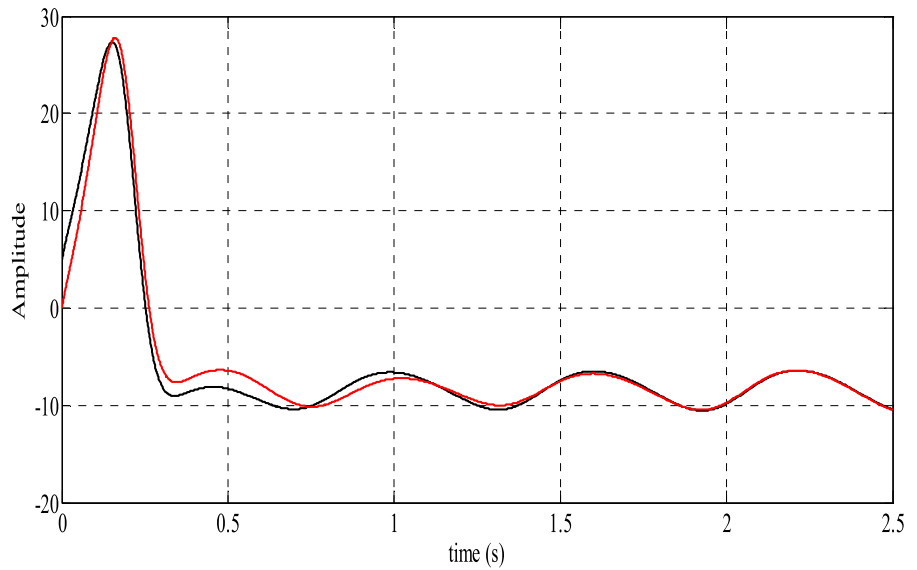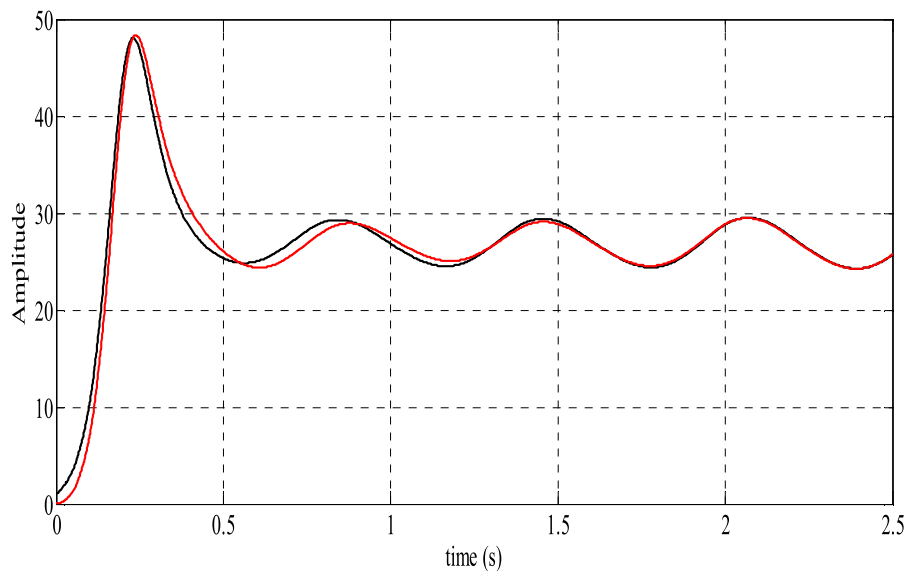mode observer. (Color
figure online)
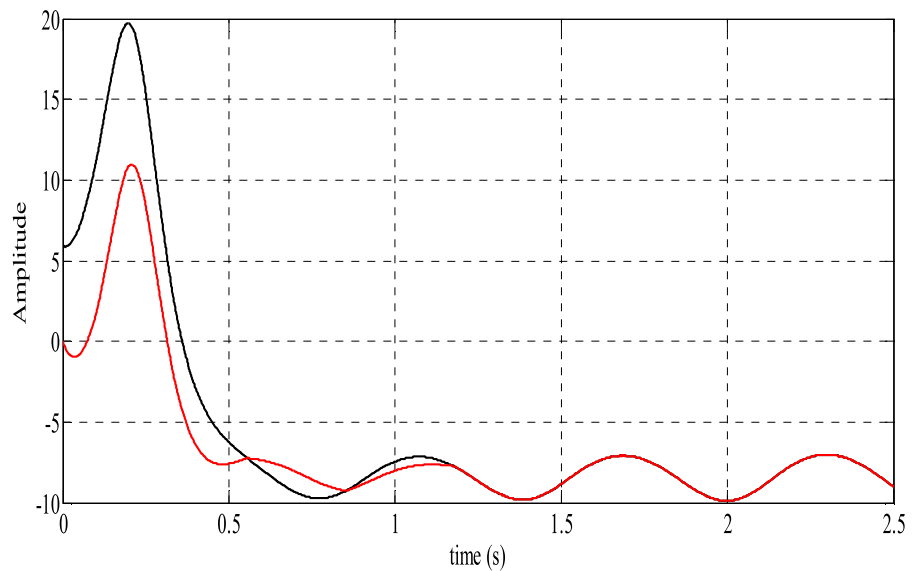
$e_i(t) = x_i(t) - \hat{x}_{\mathrm{img}}(t)$, $i = 1, 2, 3$. Obviously, we have $\tilde{e}_1(t) = e_1(t)$. The switching logic variables E_1 and E_2 obey to the following rules: $E_i = 1$ if $\|\tilde{x}_i(t) - x_i(t)\| = 0$ else $E_i = 0$, $i = 1, 2$. The observer gains are taken as $k_1 = k_2 = k_3 = 5$. Figures 8, 9 and 10 plot the estimated variables resulting from the sliding mode observer. Results obtained by the

proposed impulsive observer are much better as clearly shown in Fig. 11 where the estimation error of the proposed method is compared with the estimation error provided by the sliding mode observer. Error criteria J_{imp} for the proposed impulsive observer and J_{mg} for the sliding mode observer are evaluated as follows

$$J_{\text{imp}} = \frac{1}{N} \sum_{i=0}^{N} \sqrt{\left(x_1(t_{\text{si}}) - \hat{x}_1(t_{\text{si}})\right)^2 + \left(x_2(t_{\text{si}}) - \hat{x}_2(t_{\text{si}})\right)^2 + \left(x_3(t_{\text{si}}) - \hat{x}_3(t_{\text{si}})\right)^2}$$

$$J_{\text{mg}} = \frac{1}{N} \sum_{i=0}^{N} \sqrt{\left(x_1(t_{\text{si}}) - \hat{x}_{1\text{mg}}(t_{\text{si}})\right)^2 + \left(x_2(t_{\text{si}}) - \hat{x}_{2\text{mg}}(t_{\text{si}})\right)^2 + \left(x_3(t_{\text{si}}) - \hat{x}_{3\text{mg}}(t_{\text{si}})\right)^2}$$

where N is the number of simulations points at sampling instants t_{si}, $i = 0, 1, \ldots, N$. We get $J_{\text{imp}} = 1.61155$ and $J_{\text{mg}} = 1.9110$. This confirms the superiority of the proposed impulsive observer. The convergence time of the proposed observer is chosen almost arbitrarily and independently of the system initial conditions. In contrast, the convergence time of the sliding mode observer, or of any other finite-time observers, is,

Fig. 9 State variable x_2 (in black color) and its estimate $\hat{x}_{2\text{mg}}(t)$ (in red color) resulting from the sliding mode observer. (Color figure online)

Fig. 10 State variable x_3 (in black color) and its estimate $\hat{x}_{3\text{mg}}(t)$ (in red color) resulting from the sliding mode observer. (Color figure online)

Fig. 11 Synchronization errors resulting from the proposed observer for $\delta = 0.5s$, $\alpha = 0.995$ and $x(0) = [6 \quad 5 \quad 1]^T$ (in black color) and from the sliding mode observer (in red color). **a** $e_1(t)$, **b** $e_2(t)$, **c** $e_3(t)$. (Color figure online)
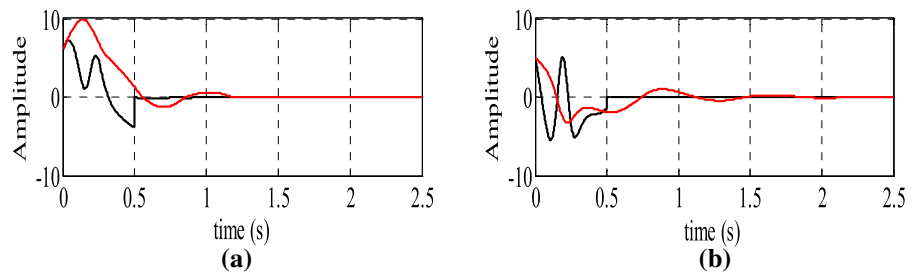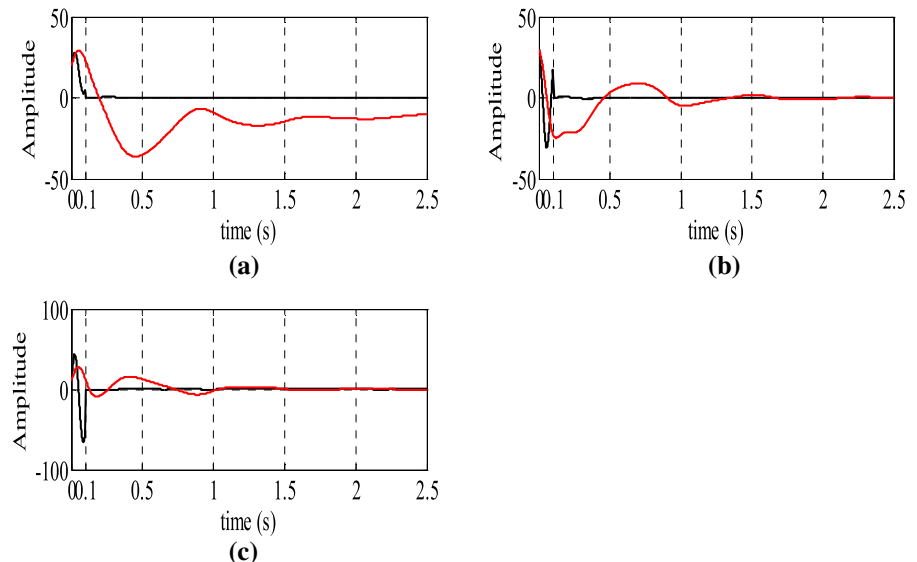

Fig. 12 Synchronization errors resulting from the proposed observer (in black color) for $\delta = 0.1s$, $\alpha = 0.995$ and $x(0) = [20 \quad 30 \quad 10]^T$ and from the sliding mode observer (in red color). **a** $e_1(t)$, **b** $e_2(t)$, **c** $e_3(t)$. (Color figure online)

in general, not known and depends on the initial conditions. Only an upper bound can be estimated. Figures 12 and 13 plot the trajectories of the estimation error with $x(0) = [60 \quad 30 \quad 10]^T$, for $t_1 = 0.1s$ and $t_1 = 1s$, respectively. We obtain $J_{imp} = 2.2986$ and $J_{mg} = 18.5951$ for $t_1 = 0.1s$ and $J_{imp} = 11.7153$ and $J_{mg} = 18.5951$ for $t_1 = 1s$. In both cases, the proposed observer works well even if the initial conditions are very large and converges instantaneously at the predefined time t_1 since $e_i(t) = x_i(t) - \hat{x}_i(t) = 0$ for $t \geq t_1$. However, this is not the case for the sliding mode observer. In order to obtain a rapid conver-

gence, the sliding mode observer requires large output injection gain. However, this would cause chattering phenomena and significant transient peaks. The proposed impulsive observer converges accurately in a predefined time without increasing the output injection gain. We also tested the performance of the proposed impulsive observer to different values of α. The values $\alpha = 0.95$ ($0 < \alpha < 1$) and $\alpha = 1.02$ ($1 \leq \alpha < 2$) are chosen so that the responses of the fractional-order Lorenz system remain bounded. For $\alpha = 0.95$, the LMIs given by (47) are solved by pole placement method in LMI region defined by $\rho_1 = 0.5$

Fig. 13 Synchronization errors resulting from the proposed observer (in black color) for $\delta = 1s$, $\alpha = 0.995$ and $x(0) = [20 \quad 30 \quad 10]^T$ and from the sliding mode observer (in red color). **a** $e_1(t)$, **b** $e_2(t)$, **c** $e_3(t)$. (Color figure online)
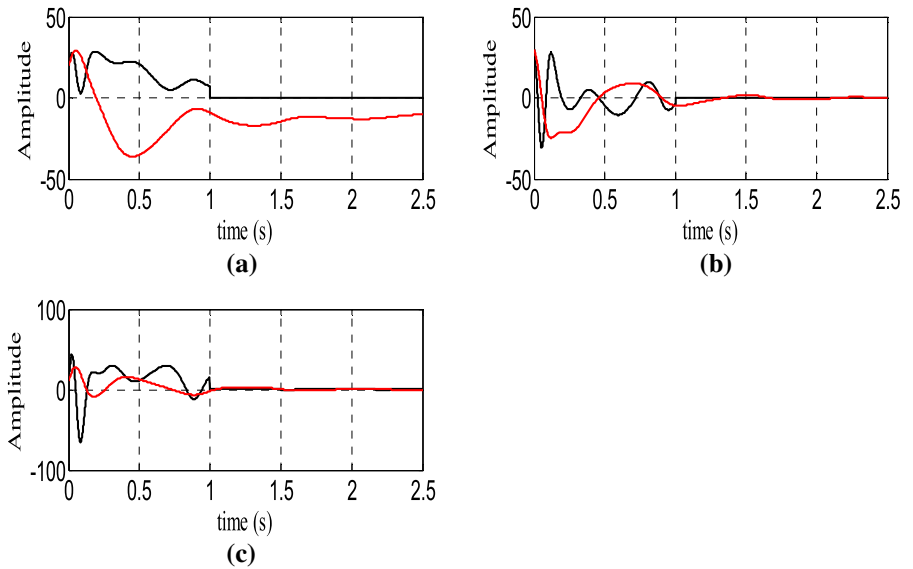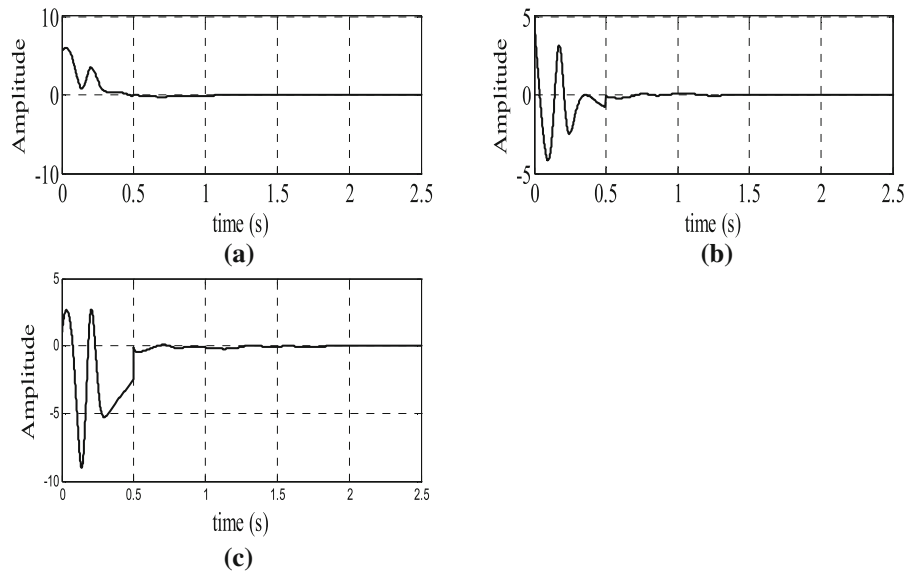

Fig. 14 Synchronization errors resulting from the proposed observer for $\delta = 0.1s$, $\alpha = 0.95$ and $x(0) = [6 \quad 5 \quad 1]^T$. **a** $e_1(t)$, **b** $e_2(t)$, **c** $e_3(t)$

and $\rho_2 = 0.7$. For $\alpha = 1.02$, the LMIs given by (48) with (49) and (50) are solved by pole placement method in LMI region defined by $\rho_1 = 15$ and $\rho_2 = 15.7$. Computer simulations are performed for $t_1 = 0.3s$ and for the initial conditions of the system $x_1(0) = 6$, $x_2(0) = 5$, $x_3(0) = 1$, while the initial conditions of the observer are fixed to zero. From the simulation results illustrated in Figs. 14, 15 and 16 almost zero synchronization errors have been achieved in finite time $t_1 = 0.3s$ which confirms that the proposed impulsive observer works well for different values of α.

4.2 Observer with unknown input in a secure data communication

Below, we present the application of the proposed observer with unknown input in a secure communication scheme. A fractional chaos-based secure communication scheme consists of an emitter and a transmitter as illustrated in Fig. 17. At the emitter side, the fractional-order Lorenz chaotic system (76) represented in the Takagi–Sugeno form (79) is used for masking the secret message. The unknown input $d(t)$ represents the secret message to be confidentially trans-

Fig. 15 True state variables (in black color) and its estimates (in red color) resulting from the proposed observer with $\delta = 0.3s$, $\alpha = 1.02$ and $x(0) = [20 \quad 15 \quad 10]^T$, **a** $x_1, \hat{x}_1$, **b** $x_2, \hat{x}_2$, **c** $x_3, \hat{x}_3$. (Color figure online)
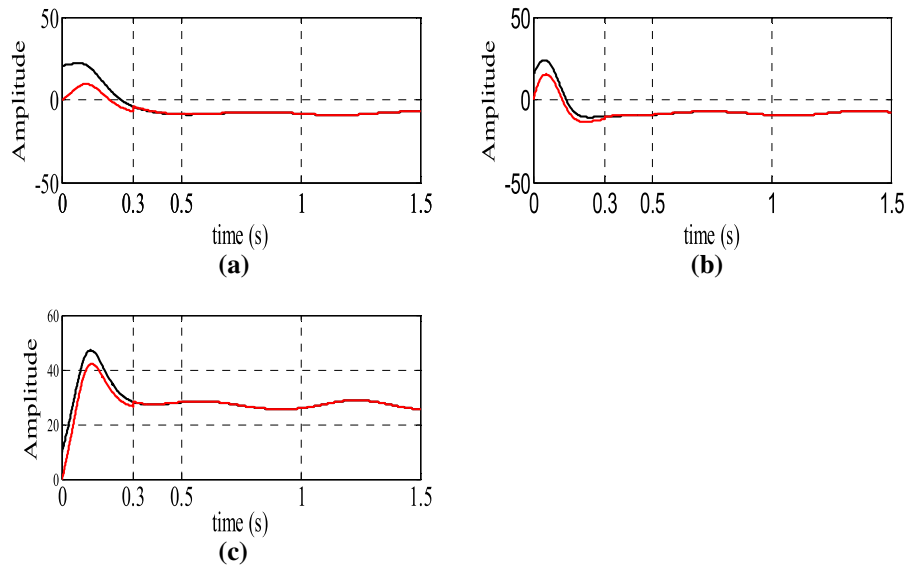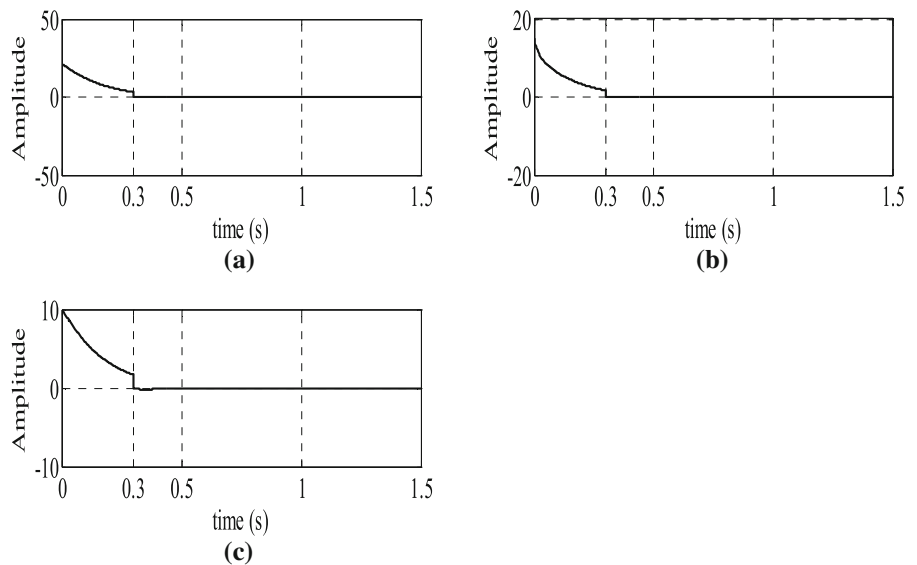
Fig. 16 Synchronization errors resulting from the proposed observer with $\delta = 0.3s$, $\alpha = 1.02$ and $x(0) = [20 \quad 15 \quad 10]^T$. **a** $e_1(t)$, **b** $e_2(t)$, **c** $e_3(t)$

mitted from the emitter to the receiver trough a public channel. The secret message is included in the chaotic dynamic and also added in the output $y(t)$ as given by (23). The emitter plays the role of an encoder. At the receiver side, the proposed unknown input impulsive observer (52) plays the role of a decoder. The goal is to show that using the proposed observer, the transmitted message can be accurately recovered by the receiver in finite time; after that, the synchronization between the emitter and the receiver is achieved. As has been pointed out in [35], the message can only be recov-
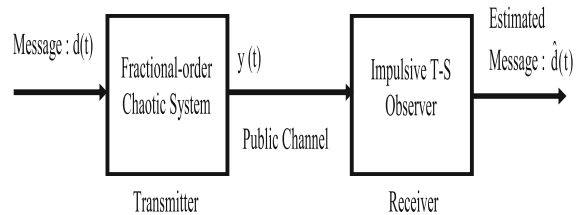
Fig. 17 Fractional-order chaos-based secure data communication scheme

ered with complete integrity if the synchronization is performed in a relatively small finite time.

The matrices R_1, R_2 and V are taken as

$$R_1 = \begin{bmatrix} 1 \\ -1 \\ 1.2 \end{bmatrix}, \quad R_2 = \begin{bmatrix} 1 \\ 1.5 \\ 1 \end{bmatrix}, \quad V = \begin{bmatrix} 1 & 1 \end{bmatrix} \quad (87)$$

Let $\delta = t_1 = 0.3s$ be the synchronization delay. In order to avoid information loss, the message to be transmitted is delayed and is taken as

$$d(t) = \begin{cases} 0 & t < t_1 \\ 0.1\sin(5t) & t \geq t_1 \end{cases}$$

Assumptions 2 and 3 are well satisfied. The order derivative is taken as $\alpha = 0.996$, and the system initial conditions are $x_1(0) = 6$, $x_2(0) = 5$, $x_3(0) = 1$. The two LMI regions $\tilde{\Omega}_1$ and $\tilde{\Omega}_2$ are chosen as ($\rho_1 = 1$, $\sigma_1 = 10$) and ($\rho_2 = 3$, $\sigma_2 = 10$), respectively. Using the YALMIP/MATLAB toolbox, the LMIs (70) and (71) with the equality constraint (55) and (56) are shown to be feasible. The recovered message is obtained as

$$\hat{d}(t) = V^+ \left(y(t) - \hat{y}(t) \right)$$
$$\hat{y}(t) = C\hat{x}(t) \quad (88)$$

where V^+ denotes the pseudoinverse of V. In Fig. 18 are reported the trajectories of the state variables $x_i(t)$ and their estimates $\hat{x}_i(t)$, $i = 1, 2, 3$, and the corre-

Fig. 18 Case with unknown input with $\delta = 0.3s$ and $\alpha = 0.996$: state variable time responses of the system (in black color) and the observer (in red color). **a** $x_1(t)$, $\hat{x}_1(t)$, **b** $x_2(t)$, $\hat{x}_2(t)$, **c** $x_3(t)$, $\hat{x}_3(t)$. (Color figure online)
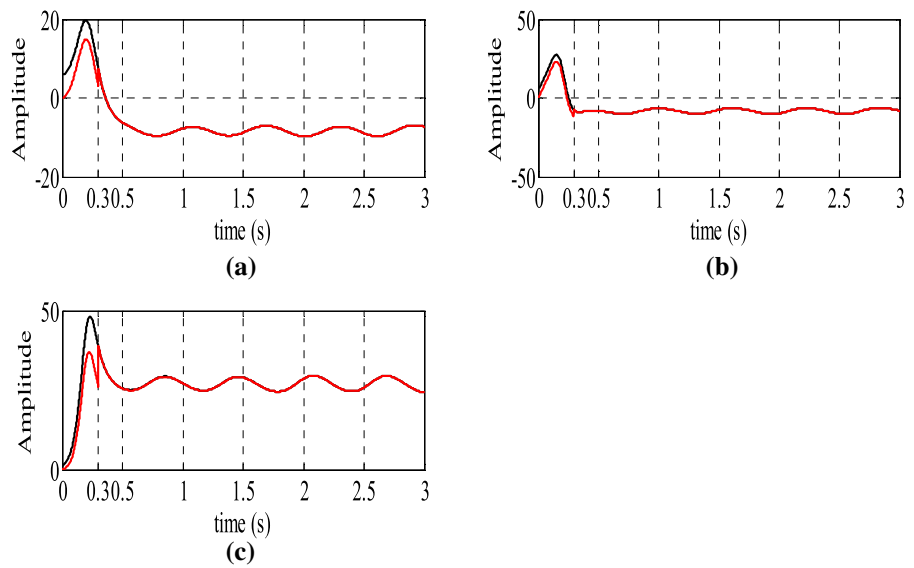

Fig. 19 Case with unknown input with $\delta = 0.3s$ and $\alpha = 0.996$: estimation errors. **a** $e_1(t) = x_1(t) - \hat{x}_1(t)$, **b** $e_2(t) = x_2(t) - \hat{x}_2(t)$, **c** $e_3(t) = x_3(t) - \hat{x}_3(t)$
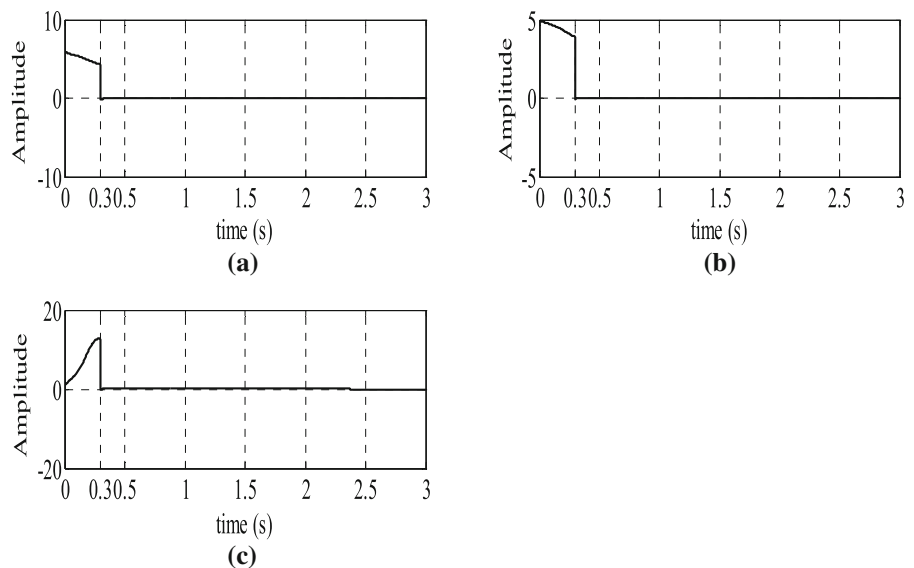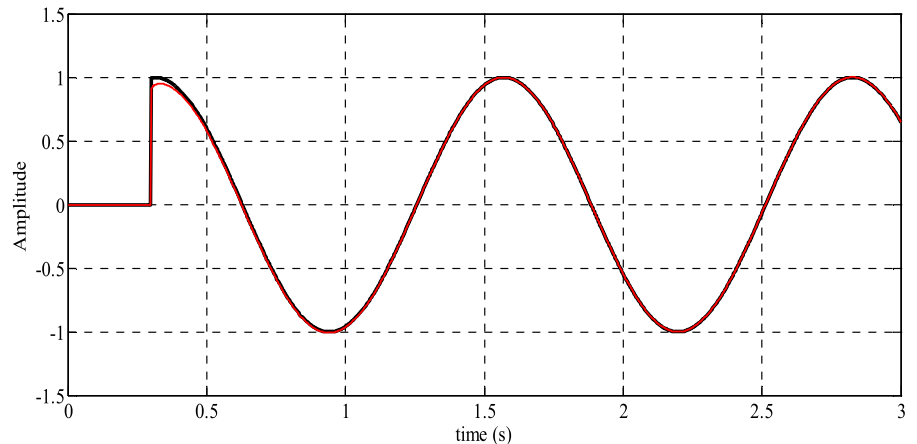
Fig. 20 Case with unknown input with $\delta = 0.3s$ and $\alpha = 0.996$: hidden message $d(t)$ and its estimate $\hat{d}(t)$

sponding estimation errors are shown in Fig. 19. From these simulation results, we check that the unknown input does not affect the observation error, and thus, the decoupling between the unknown input and the estimation of the state variables is successful, and then, the zero synchronization error is achieved after the time instant t_1. In addition to the estimation of the state variables, the proposed impulsive observer can also reconstruct the unknown input. The original message $d(t)$ and its estimate $\hat{d}(t)$ are plotted in Fig. 20. The obtained simulation results show the almost exact reconstruction of the unknown input.

5 Conclusion

In this paper, the design of predefined finite convergence time impulsive observer for nonlinear fractional-order chaotic systems is addressed. The T–S fuzzy representation of the nonlinear system subjected to an unknown input is used. The T–S model exactly describes the nonlinear system as has been illustrated with the fractional-order chaotic Lorenz system. The exact and finite-time reconstruction of the state variables and the unknown input were possible thanks to a impulsive state observer update. We treated both cases without and with the presence of the unknown input. In both cases, the convergence of the proposed observer is established using the LMI formulation. Simulation results clearly illustrate the advantage of the proposed impulsive observer in a secure data communication application. The present works can deserve future research directions. First, in the proposed work, we assumed that the premise variables are measur-

able, which is not usually always true. The extension the case of unmeasurable premise variables would be more realistic. Second, we considered a common output for all linear local models in the T–S representation. It would be worth studying the case where each output is defined for each local model. It is also interesting to study the robustness of the proposed impulsive observer with respect to output noise and modeling uncertainties. Other points worth studying concern the extension of the impulsive observer to other more complex fractional-order chaotic systems such as hyperchaotic systems, non-commensurate fractional-order chaotic systems and fractional-order neural network chaotic systems. Future works are oriented in these directions.

References

1. Monje, C.A., Chen, Y.Q., Vinagre, B.M., Xue, D., Feliu, V.: Fractional-Order Systems and Control: Fundamentals and Applications. Springer, Berlin (2010)
2. Azar, A.T., Radwan, A.G., Vaidyanathan, S.: Fractional-Order Systems Optimization, Control, Circuit Realizations and Applications. Academic Press, London (2018)
3. Caponetto, R., Dongola, G., Fortuna, L., Petras, I.: Fractional Order Systems: Modeling and Control Applications. World Scientific Series on Nonlinear Science Series A. World Scientific, London (2010)

4. Sun, H.H., Abdelwahab, A.A., Onaral, B.: Linear approximation of transfer function with a pole of fractional power. IEEE Trans. Autom. Control **29**(5), 441–444 (1984)

5. Djamah, T., Djennoune, S., Bettayeb, M.: Diffusion processes identification in cylindrical geometry using fractional models. Phys. Scr. **T136**, 014013 (2009)

6. Adolfsson, K., Enelund, M., Olsson, P.: On the fractional order model of viscoelasticity. Mech. Time-Depend. Mater. **9**(1), 15–34 (2005)

7. Elwakil, A.S.: Fractional-order circuits and systems: an emerging interdisciplinary research area. IEEE Circuits Syst. Mag. **10**(4), 40–50 (2010)

8. Podlubny, I.: Fractional-order systems and $PI^\lambda D^\mu$-controllers. IEEE Trans. Autom. Control **44**(1), 208–214 (1999)

9. Petras, I.: Fractional-Order Nonlinear Systems. Springer, Heidelberg (2011)

10. Azar, A.T., Taher, A., Vaidyanathan, S., Ouannas, A.: Fractional-Order Control and Synchronization of Chaotic Systems. Studies in Computational Intelligence. Springer, Berlin (2017)

11. Li, R.-G., Wu, H.-N.: Secure communication on fractional-order chaotic systems via adaptive sliding mode control with teaching–learning–feedback-based optimization. Nonlinear Dyn. **95**(2), 1221–1243 (2019)

12. Kassim, S., Hamiche, H., Megherbi, O., Djennoune, S., Bettayeb, M.: A novel secure image transmission scheme based on synchronization of fractional-order discrete-time hyperchaotic systems. Nonlinear Dyn. **88**(4), 2473–2489 (2017)

13. Hamiche, H., Kassim, S., Megherbi, O., Djennoune, S., Bettayeb, M.: Secure digital data communication based on fractional-order chaotic maps. In: Chapter Book in Advanced Synchronization Control and Bifurcation of Chaotic Fractional-Order Systems. IGI Global, pp. 438–467 (2018)

14. Pecora, L.M., Carrol, T.L.: Synchronization in chaotic systems. Phys. Rev. Lett. **64**(8), 821–824 (1990)

15. Behinfaraz, R., Badamchizadeh, M.A., Rikhtegar Ghiasi, A.: An approach to achieve modified projective synchronization between different types of fractional-order chaotic systems with time-varying delays. Chaos Solitons Fractals **78**, 95–106 (2015)

16. Zhang, W., Cao, J., Wu, R., Alsaadi, F.E., Alsaedi, A.: Lag projective synchronization of fractional-order delayed chaotic systems. J. Frankl. Inst. **356**(3), 11522–1534 (2019)

17. Luo, S., Li, S., Tajaddodianfar, F.: Adaptive chaos control of the fractional-order arch MEMS resonator. Nonlinear Dyn. **91**(1), 539–547 (2018)

18. Fenga, D., Ana, H., Zhub, H., Zhaoa, Y.: The synchronization method for fractional-order hyperchaotic systems. Phys. Lett. A **383**(13), 1427–1434 (2019)

19. Behinfaraz, R., Badamchizadeh, M.: Optimal synchronization of two different in-commensurate fractional-order chaotic systems with fractional cost function. Complexity **21**(S1), 401–416 (2016)

20. Jin-Gui, L.: A novel study on the impulsive synchronization of fractional-order chaotic systems. Chin. Phys. B **22**(6), 060510 (2013)

21. Wang, F., Yang, Y., Hu, A., Xu, X.: Exponential synchronization of fractional-order complex networks via pinning impulsive control. Nonlinear Dyn. **82**(4), 1979–1987 (2015)

22. Srivastava, M., Ansari, S.P., Agrawal, S.K., Das, S., Leung, A.Y.T.: Anti-synchronization between identical and non-identical fractional-order chaotic systems using active control method. Nonlinear Dyn. **76**(2), 905–914 (2014)

23. Pratap, A., Raja, R., Cao, J., Rajchakit, G., Fardoun, H.M.: Stability and synchronization criteria for fractional order competitive neural networks with time delays: an asymptotic expansion of Mittag–Leffler function. J. Frankl. Inst. **356**, 2212–2239 (2019)

24. Chen, L., Cao, J., Wu, R., Machado, J.A.T., Lopes, A.M., Yang, H.: Stability and synchronization of fractional-order memristive neural networks with multiple delays. Neural Netw. **94**, 76–85 (2016)

25. Nijmeijer, H., Mareels, I.M.Y.: An observer looks at synchronization. IEEE Trans. Circuits Syst. I Fundam. Theory Appl. **44**(10), 882–890 (1997)

26. N'Doye, I., Salam, K.H., Laleg-Kirati, T.M.: Robust fractional-order proportional-integral observer for synchronization of chaotic fractional-order systems. EEE/CAA J. Autom. Sin. **6**(1), 268–277 (2019)

27. Bettayeb, M., Al-Saggaf, U.M., Djennoune, S.: High gain observer design for fractional-order non-linear systems with delayed measurements: application to synchronisation of fractional-order chaotic systems. IET Control Theory Appl. **11**(17), 3171–3178 (2017)

28. Liu, L., Liang, D., Liu, C.: Nonlinear state-observer control for projective synchronization of a fractional-order hyperchaotic system. Nonlinear Dyn. **69**(4), 1929–1939 (2012)

29. Liu, H., Pan, Y.P., Li, S., Chen, Y.: Synchronization for fractional-order neural networks with full/under-actuation using fractional-order sliding mode control. Int. J. Mach. Learn. Cybern. **9**(7), 1219–1232 (2018)

30. Li, Y., Hou, B.: Observer-based sliding mode synchronization for a class of fractional-order chaotic neural networks. Adv. Differ. Equ. Springer Open, Published on: 24 April 2018, 2018:146 (2018)

31. Azar, A.T., Serranot, F.E., Vaidyanathan, S.: Sliding mode stabilization and synchronization of fractional order complex chaotic and hyperchaotic systems. In: Azar, A.T., Radwan, A.G., Vaidyanathan, S. (eds.) Chapter 10 in Advances in Nonlinear Dynamics and Chaos (ANDC), Mathematical Techniques of Fractional Order Systems, pp. 283–317. Elsevier, Amsterdam (2018)

32. Belkhatir, Z., Laleg-Kirati, T.M.: High-order sliding mode observer for fractional commensurate linear systems with unknown input. Automatica **82**, 209–217 (2017)

33. Muthukumar, P., Balasubramaniam, P., Ratnavelu, K.: Sliding mode control design for synchronization of fractional order chaotic systems and its application to a new cryptosystem. Int. J. Dyn. Control **5**(1), 115–123 (2017)

34. Mofid, O., Mobayen, S., Khooban, M.-H.: Sliding mode disturbance observer control based on adaptive synchronization in a class of fractional-order chaotic systems. Int. J. Adapt. Control Signal Process. **33**(3), 462–474 (2019)

35. Anguiano-Gijon, C.A., Munoz-Vaequez, A.J., Sanchez-Torres, J.D., Romero-Galvan, G., Martinez-Reyes, F.: On predefined-time synchronization of chaotic systems. Chaos Solitons Fractals **122**, 172–178 (2019)

36. Levant, A.: High-order sliding modes, differentiation and output feedback control. Int. J. Control **76**(9/10), 924–941 (2003)

37. Shtessel, Y., Edwards, C., Fridman, L., Levant, A.: Sliding Mode Control and Observation. Birkhauser, Springer, Heidelberg (2014)

38. Raff, T., Allgower, F.: An impulsive observer that estimates the exact state of a linear continuous-time system in predetermined finite time. In: Proceedings of the 15th Mediterranean Conference on Control and Automation, Athens, Greek, T19-014 (2007)

39. Raff, T., Allgower, F.: Observers with impulsive dynamical behavior for linear and nonlinear continuous-time systems. In: Proceedings of the 46th IEEE Conference on Decision and Control, New-Orleans, LA, USA, pp. 4287–4292 (2007)

40. Djennoune, S., Bettayeb, M., Al Saggaf, U.M.: Exact impulsive observer with predetermined finite-time convergence of fractional-order systems with unknown input. In: Proceedings of International Conference on Fractional Differentiation and Its Applications (ICFDA), Amman, Jordania (2018)

41. Takagi, T., Sugeno, M.: Fuzzy identification of systems and its applications to modeling and control. IEEE Trans. Syst. Man Cybern. **15**(1), 116–132 (1985)

42. Boukhris, A., Mourot, D., Ragot, J.: Nonlinear dynamical systems identification: a multi-model approach. Int. J. Control **72**(7–8), 591–604 (1999)

43. Tanaka, K., Wang, H.O.: Fuzzy Control Systems Design and Analysis. A Linear Matrix Inequality Approach. Wiley, New York (2001)

44. Ohtake, H., Tanaka, K., Wang, H.O.: Fuzzy modeling via sector nonlinearity concept. Integr. Comput.-Aided Eng. **10**(4), 333–341 (2003)

45. Chadli, M.: An LMI approach to design observer for unknown inputs Takagi–Sugeno fuzzy models. Asian J. Control **12**(4), 524–530 (2010)

46. Ichalal, D., Marx, B., Ragot, J., Maquin, D.: Advances in observer design for Takagi–Sugeno systems with unmeasurable premise variables. In: 20th Mediterranean Conference on Control and Automation, MED 2012, July 2012. Barcelona, Spain, pp. 848–853 (2012)

47. Liu, H., Pan, Y., Li, S., Chen, Y.: Adaptive fuzzy backstepping control of fractional-order nonlinear systems. IEEE Trans. Syst. Man Cybern. Syst. **47**(8), 2209–2217 (2017)

48. Duan, R., Li, J.: Observer-based controller design for fractional-order T–S fuzzy systems with Markovian jump and multiplicative sensor noises. In: Proceedings of the 37th Chinese Control Conference (CCC), July 25–27, 2018, Wuhan, China (2018)

49. Muthukumar, P., Balasubramaniam, P., Ratnavelu, K.: T–S fuzzy predictive control for fractional order dynamical systems and its applications. Nonlinear Dyn. **86**(2), 751–763 (2016)

50. Ji, Y., Yang, L., Qiu, J.: Robust stabilization of uncertain fractional-order systems based on T–S fuzzy model. In: Proceedings of 34th Chinese Control Conference (CCC), July 28–30, 2015 Hangzhou, China (2015)

51. Wang, L., Ni, J., Yang, C.: Synchronization of different uncertain fractional-order chaotic systems with external disturbances via T–S Fuzzy model. J. Funct. Spaces 2018 (ID 2793673) https://doi.org/10.1155/2018/2793673 (2018)

52. Matouk, A.E.: Chaos synchronization of a fractional-order modified van der Pol–Duffing system via new linear control, backstepping control and Takagi–Sugeno fuzzy approaches. Complexity **21**(S1), 116–124 (2016)

53. Lu, J.G., Chen, Y.Q.: Robust stability and stabilization of fractional-order interval systems with the fractional-order α: the $0<\alpha<1$ case. IEEE Trans. Autom. Control **55**(1), 182–188 (2010)

54. Sabatier, J., Moze, M., Farges, C.: LMI stability conditions for fractional-order systems. Comput. Math. Appl. **59**(5), 1594–1609 (2010)

55. Li, Y., Li, J.: Stability analysis of fractional-order systems based on T–S fuzzy model with the fractional-order α: $0<\alpha<1$. Nonlinear Dyn. **78**(4), 2909–2919 (2014)

56. Li, Y., Chen, Y.Q., Podlubny, I.: Mittag–Leffler stability of fractional order nonlinear dynamic systems. Automatica **45**(8), 1965–1969 (2009)

57. Podlubny, I.: Fractional Differential Equations. Academic Press, New York (1999)

58. Kilbas, A.A., Srivastava, H.M., Trujillo, J.J.: Theory and application of fractional differential equations. In: van Mill, J. (ed.) North Holland Mathematics Studies. Elsevier, Amsterdam (2006)

59. Matignon, D.: Stability properties for generalized fractional differential systems. In: Proceedings of the Fractional Differential Systems: Models, Methods and Applications, pp. 145–158 (1998)

60. Matignon, D., D'Andrea-Novel, B.: Some results on controllability and observability of infinite-dimensional fractional differential systems. In: Proceedings of Computational Engineering in Systems Applications, Lille, France, pp. 952–956 (1996)

61. Zhang, X., Wang, H., Lv, Y.: State transition matrix of linear time-varying fractional order systems. In: 2017 29th Chinese Control and Decision Conference (CCDC), 28–30 May 2017, Chongqing, China (2017)

62. Eckert, M., Nagatou, K., Rey, R., Stark, O., Hohmann, S.: Solution of time-variant fractional differential equations with a generalized Peano-Baker series. IEEE Control Syst. Lett. **3**(1), 29–84 (2019)

63. Lofberg, J.: Yalmip: a toolbox for modeling and optimization in Matlab. In: IEEE International Symposium on Computer Aided Control Systems Design, pp. 284–289 (2004)

64. Chilali, M., Gahinet, P.: H_∞ design with pole placement constraints: an LMI approach. IEEE Trans. Autom. Control **41**(3), 358–367 (1996)

65. Patton, R., Chen, J., Lopez-Toribio, C.: Fuzzy observers for non-linear dynamic systems fault diagnosis. In: 37th IEEE Conference on Decision and Control, Tampa, Florida (1998)